Automated EEG analysis of epilepsy: A review

U. Rajendra Acharya [a,b,*], S. Vinitha Sree [c], G. Swapna [d], Roshan Joy Martis [a], Jasjit S. Suri [e,f]

[a] Department of Electronics and Computer Engineering, Ngee Ann Polytechnic, Singapore 599489, Singapore
[b] Department of Biomedical Engineering, Faculty of Engineering, University of Malaya, Malaysia
[c] Visiting Scientist, Global Biomedical Technologies, CA, USA
[d] Department of Applied Electronics & Instrumentation, Government Engineering College, Kozhikode, Kerala 673 005, India
[e] Department of Biomedical Engineering (Affl.), Idaho State University, Pocatello, ID, USA
[f] Point of Care Division, CTO, Global Biomedical Technologies, Inc., 208 Otter Glen CT, Roseville, CA 95661, USA

ABSTRACT

Epilepsy is an electrophysiological disorder of the brain, characterized by recurrent seizures. Electroencephalogram (EEG) is a test that measures and records the electrical activity of the brain, and is widely used in the detection and analysis of epileptic seizures. However, it is often difficult to identify subtle but critical changes in the EEG waveform by visual inspection, thus opening up a vast research area for biomedical engineers to develop and implement several intelligent algorithms for the identification of such subtle changes. Moreover, the EEG signals are nonlinear and non-stationary in nature, which contribute to further complexities related to their manual interpretation and detection of normal and abnormal (interictal and ictal) activities. Hence, it is necessary to develop a Computer Aided Diagnostic (CAD) system to automatically identify the normal and abnormal activities using minimum number of highly discriminating features in classifiers. It has been found that nonlinear features are able to capture the complex physiological phenomena such as abrupt transitions and chaotic behavior in the EEG signals. In this review, we discuss various feature extraction methods and the results of different automated epilepsy stage detection techniques in detail. We also briefly present the various open ended challenges that need to be addressed before a CAD based epilepsy detection system can be set-up in a clinical setting.

© 2013 Elsevier B.V. All rights reserved.

1. Introduction

Epilepsy is the most common neurological disorder affecting 50 million people world-wide, 85% of which belong to the developing countries. Around 2.4 million new cases occur every year globally. At least 50% of the epileptic cases begin at childhood or adolescence [124]. Sudden onset may also be seen in geriatric population (people above the age of 65) [92]. Epileptic people are two or three times more likely to die prematurely when compared to a normal person [124]. Hence, study of epilepsy has always been an utmost importance in the biomedical field of research.

Epilepsy is a chronic brain disorder, characterized by seizures, which can affect any person at any age. It is characterized by recurrent convulsions over a time-period. The episodes may vary as low as once in a year to frequent fits occurring several times per day. Epilepsy and seizure disorders are not the same; in other words all the seizures are not epileptic fits. Epilepsy is characterized by unprovoked seizures due the involvement of the central nervous system. It is due to the process of 'epileptogenesis' [24] where normal neuronal network abruptly turns into a hyper-excitable network, affecting mostly the cerebral cortex. It is therefore highly unpredictable and its risk is much immeasurable. On the other hand, non-epileptic seizure disorders could be due to several measurable causes, such as stroke, dementia, head injury, brain infections, congenital birth defects, birth-related brain injuries, tumors and other space occupying lesions. The resulting type of epilepsy is called as *secondary* or *symptomatic epilepsy*. For secondary epilepsy, preventive measures can be adopted according to the various causes. It is interesting to note that for more than 60% of cases, no definite cause can be ascertained. This broader type of epilepsy is known as *idiopathic* or *primary epilepsy*. It is therefore not preventable, but treatable with antiepileptic medications.

The epileptic seizures occur because of the malfunctioning of the electrophysiological system of the brain, which causes sudden excessive electrical discharge in a group of brain cells (i.e. neurons) present in the cerebral cortex. Involvement of cerebral cortex leads to abnormalities of motor functions causing jerky (tonic-clonic) spasms of muscles and joints. The underlying physiology is the hyper synchronous activity of neurons causing altered and inappropriate changes in sensory and motor activity. Instead of

controlled discharge of electrical energy, there is an abrupt and huge surge of energy by the brain cells causing the epileptic seizures. The seizures show large variations in properties. A seizure can be seen as a minute muscle twitch to severe, generalized and prolonged convulsions. Recurrent and suddenly occurring seizures are dangerous and can lead to life-threatening situations [20]. The characteristics of the seizure depend on the (i) specific region involved in the brain, (ii) extent of abnormal electrical discharge, and (iii) its spread.

The human knowledge of the functioning of the brain is still insufficient to understand the properties of an epileptic brain [51]. Possible temporary symptoms of epilepsy are loss of mindfulness, almost undetectable abnormalities in the movement pattern, very mild twitching of muscles, disturbances in visual, auditory, gustatory senses and mood and many others are often beyond manual recognition. Further, epileptic seizures usually begin and end spontaneously without any external interference and could remain unnoticed. Hence, detecting and measuring epileptic seizures should be a continuous process, and therefore, involves several engineering challenges. In Section 1.1, we present the different methods currently used to detect epilepsy. In Section 1.2, we briefly discuss on the use of EEG signals for detection of epilepsy by the identification of various associated EEG activities (pre-ictal, interictal, and ictal) that occur in and around seizures.

1.1. Methods for detection of epilepsy

The occurrence of a seizure may not always be due to epilepsy since about 10% of the people in the world have one seizure in their lifetime. Chemical imbalances like low blood sugar, low oxygen, abnormal sodium, calcium, and potassium in blood can also cause seizures. These non-epileptic seizures (also known as pseudoseizures, phychogenic or cryptogenic seizures) are episodic events and not related to epilepsy. However, they are abnormal electrical activities in the brain. Hence, detecting non-epileptic pseudoseizures amidst the plausibility of seizures due to either primary and/ or secondary epilepsies could be very challenging. Clinically speaking, if two or more unprovoked seizures occur, we can suspect that the cause may be epilepsy. If seizure is due to epilepsy, the detection of epilepsy at its onset is very beneficial for initiating early treatment with antiepileptics for improving the quality of life and safety of epileptic people. It is the unpredictability of the seizures that mainly causes physical hazards, due to accidents, such as drowning (if it occurs while swimming or bathing), burns, and head injury.

Research studies about the mechanisms behind seizures mainly concentrate on studying neural components like neurotransmitter receptors or specific ionophores (protein structure which regulate the flow of ions across cell membrane). Osorio et al. [76] reported that it is possible to detect epileptic seizure by studying seizure intensity. There was a detection latency of 2.1 s. The authors later developed a real-time epilepsy detection and intervention scheme by direct electrical stimulation of the brain [77]. Niederhoefer et al. [72] developed algorithms to detect the onset of epileptic seizures using informative measures extracted from raw data. These epilepsy detection methods employ biological parameters for the analysis of seizure characteristics. However, the better approach is to analyze the patterns of the Electroencephalogram (EEG) signals because they are a direct reflection of the electrophysiological conditions of the brain at a given timestamp. Clinical diagnosis of epilepsy requires detailed history and also neurological examinations along with blood tests and sometimes cerebrospinal fluid tests for checking the chance of associated causes, e.g. biochemical imbalances, as mentioned before. Imaging techniques like CT (Computerized Tomography) or MRI (Magnetic Resonance Imaging) scans may be used to check for any structural abnormalities (such as tumors, abnormal blood vessels, and ischemia) in the brain, which may be causing seizures that may not be due to epi-

lepsy. However, the most common effective diagnostic method for the detection of epilepsy is the analysis of EEG signals.

1.2. EEG analysis for epilepsy detection

The EEG directly records the electrical activities of the cerebral cortex through the electrodes placed on the scalp. It actually measures the electrical potentials of the dendrites of the neurons adjacent to cortical surface. Using EEG analysis, Wackermann et al. [119] did the characterization of sleep phenomena, Stam et al. [105] studied about Creutzfeldt–Jakob disease, Stam et al. [106] studied nonlinear changes in encephalopathies, and Schraag et al. [100] monitored the depth of required anesthesia. Though these studies are not related to epilepsy, it is evident that many abnormalities related to the improper functioning of the brain can be analyzed by studying the EEG signals. The characteristics of epileptic seizures can be studied by the analysis of the recorded EEG signals. EEG signals recorded just before and during seizures contain patterns which are different from those in a normal EEG signal recorded from a normal non-epileptic person. EEG analysis can not only differentiate epileptic from normal data, but also distinguish these different abnormal stages/patterns of a seizure, such as pre-ictal (EEG changes preceding a seizure) and ictal (EEG changes during a seizure). In cases where patients have more than one seizure within a small duration, there is a stage called the interictal stage. In the common mode of epilepsy, there is a single episode of seizure. In short, pre-ictal is the stage before seizure, while interictal is the stage between two consecutive seizures. Pre-ictal or interictal EEG samples are taken from an epilepsy patient when there is no seizure. The ictal EEG data are recorded during the seizure. The electrophysiological behavior of the brain exhibits change during the shift from normal stage to pre-ictal and epileptic seizure stages. The dynamics of pre-ictal transition are highly complex. The number of involved neurons is variable ranging from tens to thousands. Even for the same patient, the duration of transition from pre-ictal to ictal stage and the participating cortical regions vary for each seizure [49,50]. During the pre-ictal stage, there is a reduction in the connectivity of neurons in the epileptogenic zone. The epileptic neurons then get isolated from the circuit [80]. These changes bring variations in the EEG signal. The isolated epileptic neurons turn idle and eventually lose the inhibitory control from neighborhood. This results in seizure, due to sudden increase in neural discharge. This further increases the variability in the EEG signal. An increase in entropy is associated with the occurrence of such abnormal electrical activity [102,1,22]. Sleigh et al. [102] showed that the changes in the entropy of EEG measures changes in the entropy occurring within the cerebral cortex of the brain.

During epilepsy, less number of independent functions and processes are active in the brain. Epileptic seizures can be clearly distinguished from non-epileptic ones by observing the EEG recordings as non-epileptic seizures have normal EEG readings. In order to achieve this goal, an efficient method of EEG signal analysis, which can provide maximum information about the condition of the brain, has to be adopted. It is possible for experienced neurophysiologists to detect epilepsy by visually scanning the EEG signals for pre-ictal, interictal and ictal activities. However, for more objective analysis and reproducible results, it is always advantageous to detect these activities from the EEG signals through some computer methods by extracting relevant features from the signals. Adeli et al. [129] launched the field of automated EEG-based diagnosis by analyzing and characterizing epileptiform discharges using wavelet transform. Their group not only proposed automated diagnosis systems for epilepsy [33–36] but also for other neurological [130] as well as psychiatric disorders such as Attention Deficit Hyperactivity Disorder [131–133], Autism Spectrum Disorder [134,135], AD [136–139], and Major Depressive Disorder [140,

141]. The scope of this review is to elaborate on the variety of Computer Aided Diagnostic (CAD) techniques that have been developed for epilepsy detection using EEG signals. Some studies focus on detecting epilepsy by classifying only the normal and ictal stages (two-class problem), and few other studies present methods to classify all three stages, namely, normal, interictal, and ictal (three-class problem). After confirming that the seizure is due to epilepsy, the next step is to detect and possibly predict the onset [47]. The onset of epileptic seizures can be predicted by detecting pre-ictal EEG signals. Again, such a prediction system requires automated classification of EEG segments in real time into three classes along with post-processing, taking into account the previous classification data and history. Another approach for prediction is detection of any EEG characteristics differing from that of the normal. This may be an indication that the pre-ictal state is being approached [22]. Thus, for both epilepsy detection and seizure onset prediction, there is a need for an automated system that can clearly differentiate normal, pre-ictal (or interictal) and epileptic stages. The recorded EEG signal is the input for such an automated system and the output is the classification label of whether the segment belongs to a normal, pre-ictal (or interictal) or epileptic stage. The two primary considerations for this detection system are the type of features to be extracted from the EEG input signal (feature extraction techniques) and the type of analysis techniques to be applied on these extracted features to detect the stage (classification techniques). In the forthcoming sections of this paper, we review these two techniques in detail and also present the results of various studies conducted in this area.

The main EEG analysis methods are time domain, frequency domain, time–frequency domain, and nonlinear methods. The functioning of the brain at the microscopic level, i.e. the interplay of neurons, is extremely nonlinear in nature since the dynamic behavior of individual neurons is decided by threshold and saturation phenomena [59]. Hence, instead of the traditional linear methods like time and frequency domain methods, nonlinear dynamics analysis methods may better suit for the analysis of the complex and nonlinear EEG waveform recorded from the brain. This paper is organized as follows. In Section 2.1, we describe the time domain, frequency domain and the time–frequency/wavelet domain techniques used for EEG analysis and for feature extraction from the EEG segments. In the same section, we elaborate on the nonlinear features that have commonly been used to quantify the normal, interictal and ictal segments of the recorded EEG signal. We discuss on the need for surrogate data analysis in Section 2.2, and the need for nonlinear analysis of EEG signals in Section 2.3. In Section 3, we review the findings of several studies that use the techniques described in Section 2.1 to classify normal and abnormal (interictal and ictal) activities in the EEG signals. We also briefly present the various open ended challenges that need to be addressed before a CAD based epilepsy detection system can be set-up in a clinical setting. We conclude the paper in Section 4.

2. Methods

2.1. EEG analysis methods

During the seventies, EEG analysis implied interpreting the EEG waveform using descriptive and heuristic methods [21]. In time, various methods have been used to analyze several subtle changes in the EEG signal. Most of the methods fall under four broad categories: (1) time domain, (2) frequency domain, (3) time–frequency domain and (4) nonlinear methods.

2.1.1. Time domain methods
The important methods for time domain analysis are *linear prediction* and *component analysis*. Fig. 1 shows the typical EEG waveforms in time domain belonging to a normal person and an epilepsy patient in the ictal and interictal states.

2.1.1.1. Linear Prediction (LP). In this method, the output of a linear system is predicted based on input $x(n)$ and previous outputs $y(n-1), y(n-2), \ldots, y(n-p)$ as shown in the following equation:

$$\hat{y}(n) = \sum_{k=1}^{p} a(k)y(n-k) + \sum_{k=0}^{N} b(k)x(n-k) \tag{1}$$

Here 'a' and 'b' are called predictor coefficients and $\hat{y}(n)$ is the estimate of $y(n)$. From Eq. (1), it is evident that the estimate is equal to a linear combination of past output values along with past and present input values. According to Pradhan and Dutt [89], LP can be used for the generation, storage, and transmission of EEG waveforms. Altunay et al. [9] utilized linear prediction error energy method to detect epileptic seizures in EEG records.

2.1.1.2. Component Analysis. Component analysis is an unsupervised method to map the data set to a feature set. Principal, linear, and independent component analyses are the methods of component analysis used in epilepsy diagnosis [26].

2.1.1.2.1. Principal Component Analysis (PCA). PCA transforms the high-dimensional data to a low-dimensional orthogonal feature (Eigenvector) subspace so that the mapping is optimum in a sum-squared error sense. Each of the orthogonal features is called a 'principal component'. The most significant variance in the data set is captured by the first principal component. The next significant variance is captured by the second principal component. The second principal component is directionally perpendicular to the first principal component. The value of the dimension of the feature space depends on the distribution of data points in the data set. In PCA, the extracted feature subspace is linear. Ghosh-Dastidar et al. [35], Subasi and Gursoy [110] and Acharya et al. [7] used PCA for the classification of epileptic EEG signals.

2.1.1.2.2. Independent Component Analysis (ICA). ICA assumes that each measured signal is a linear combination of independent signals. It decomposes multidimensional data vector linearly to statistically independent components. ICA can be effectively used to remove artifacts and to decompose EEG recorded signals into different component signals originated from different sources [57]. In the context of epilepsy detection, ICA is used to extract the independent subcomponents corresponding to epileptic seizure from the mixture of EEG signals. The extracted subcomponents are then used to train classifiers that learn the difference between normal and epileptic segments. This process is illustrated in Fig. 2. A test EEG signal can be input into a trained classifier to detect the presence of any seizure affected segments in it.

2.1.1.2.3. Linear Discriminant Analysis (LDA). Like PCA, LDA is another commonly used technique for the reduction of dimensionality. LDA causes dimensionality reduction by finding a linear combination of features which can separate two or more classes. This linear combination can serve as a linear classifier. LDA models the difference between classes of data. LDA maximizes the ratio of variance between classes to the variance within class in the data set. LDA does not change the location of the original data sets, but provides more separation between classes. Kaplan [61] studied about the time-varying spectral characteristics of the epileptic EEG waveform and computed the statistical parameters in time domain. Subasi and Gursoy [110] used the time domain methods of PCA, ICA and LDA to reduce the dimensionality of frequency domain parameters for detecting epileptic EEG.

2.1.2. Frequency domain methods
Spectral analysis is a detailed examination of information contained in the frequency domain by using statistical and Fourier Transform (FT) methods. Spectral estimation methods can be categorized as (1) the classical or non-parametric method and (2) the non-classical or parametric approach.
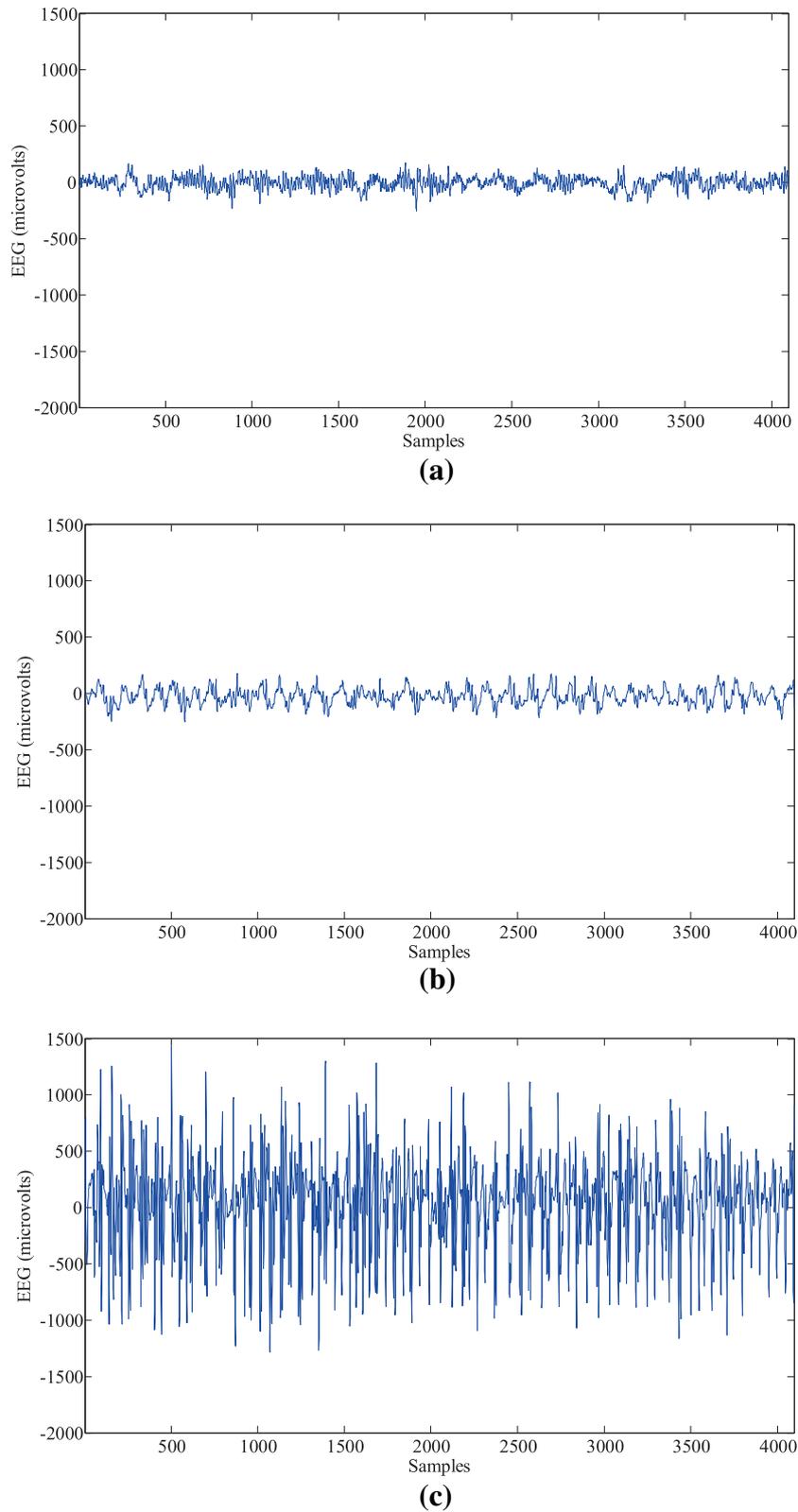
Fig. 1. Typical EEG signals (a) normal, (b) interictal and (c) ictal.

2.1.2.1. Non-parametric method. In this method, autocorrelation is initially estimated from a time sequenced data set. The next step is power spectrum estimation by applying FT to the autocorrelation sequence. The Welch method is commonly used to estimate the power spectrum of a time sequence [122]. In the Welch method, a data window is applied to each segment of the time sequence to divide the time sequence into successive blocks, and the periodogram is formed for each block, and finally the periodograms are
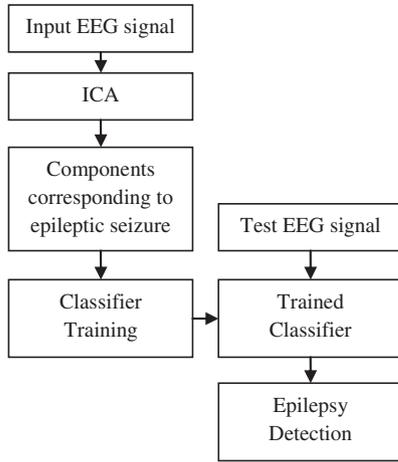
Fig. 2. Illustration of use of ICA in epilepsy detection.

averaged over time to determine the estimate of the Power Spectral Density (PSD). Let the pth windowed, zero-padded frame from the input signal x be denoted by

$$x_p(n) \cong w(n)x(n + pR), \quad n = 0, 1, \ldots, M - 1, \quad p = 0, 1, \ldots, K \quad (2)$$

where R is the window hop size and K is the number of available frames. The periodogram of the pth block is given by

$$P_{x_p,M}(w_k) = \frac{1}{M}|\text{FFT}_{N,k}(x_p)|^2 \cong \frac{1}{M}\left|\sum_{n=0}^{N-1}x_p(n)e^{-j2\pi nk/N}\right|^2 \quad (3)$$

The Welch estimate of PSD (average of periodograms across time) is given by

$$\widehat{\text{PSD}}(w_k) \cong \frac{1}{K}\sum_{p=0}^{K-1}P_{x_p,M}(w_k) \quad (4)$$

Polat and Gunes [86] used the Welch method for developing a system for two-class epilepsy detection.

2.1.2.2. Parametric method. The non-parametric method has the disadvantage of spectral leakage due to the use of windows. This is overcome by parametric or model-based power spectrum estimation methods. The parametric method also provides better frequency resolution compared to non-parametric. In this method,

Fig. 3. PSD estimation using Burgs method for normal, interictal and ictal signals shown in Fig. 1.

the signal is assumed to be a stationary random process. The signal is then modeled as the output of a filter for which white noise is the input. Then, the corresponding filter parameters are found out. There are many methods to calculate the filter parameters according to the model of the filter used. The model of the filter and hence the method used depends on the presence and absence of poles in the z-domain. The Moving Average (MA) model, the Auto Regressive (AR) model and the Auto Regressive Moving Average (ARMA) model are the three available models. Given a time series data x_t, these three models can be used to predict the future values in the series. The AR model, which can be viewed as the output of an all-pole infinite impulse response filter whose input is white noise, can be defined as

$$x_t = c + \sum_{i=1}^{a}\rho_i x_{t-i} + \varepsilon_t \quad (5)$$

where c is a constant, ε_t is white noise, and $\rho_1, \ldots, \rho_a$ are the parameters of the model. ARMA model, on the other hand, refers to a model with a autoregressive terms and b moving-average terms.

$$x_t = c + \sum_{i=1}^{a}\rho_i x_{t-i} + \varepsilon_t + \sum_{i=1}^{b}\mu_i x_{t-i} \quad (6)$$

where c is a constant, ε_t is white noise, $\rho_1, \ldots, \rho_a$ are the parameters of the AR model, and $\mu_1, \ldots, \mu_b$ are the parameters of the MA model. Burg's method is an efficient algorithm to obtain a stable AR model [115]. The AR model parameters are obtained by the minimization of both forward and backward prediction errors and the estimation of the reflection coefficient. Fig. 3 shows the PSD estimation using Burgs method for normal, interictal and ictal segments shown in Fig. 1.

2.1.3. Time–frequency domain methods
2.1.3.1. Wavelet transform. A wavelet is a small wave of finite duration and finite energy which is correlated with the EEG signal to obtain the wavelet coefficients [118]. Initially the mother wavelet (a reference wavelet) is shifted continually along the time scale to obtain a set of coefficients at all instants of time. The wavelet coefficients represent the signal in both the time and frequency domains. Next the wavelet is dilated for a different width and then normalized so as to contain the same amount of energy as the mother wavelet. Then the first process of shifting this dilated wavelet along the time scale and evaluating the corresponding set of coefficients is done. Discrete Wavelet Transform (DWT), Continuous Wavelet Transform (CWT) and Wavelet Packet Decomposition (WPD) are the three types of wavelet transforms. Jahankhani et al. [52], Sadati et al. [99], Subasi [109] and Ocak [74] used DWT in their work for automated detection of epilepsy. Acharya et al. [3] used WPD for detecting epileptic stages using Higher Order Spectra (HOS) cumulants. WPD is an extension of the DWT. In the case of DWT, in the first level, the signal is decomposed into coarse approximation coefficients by filtering it using a low-pass filter and into detail coefficients by passing it through a high-pass filter. In the subsequent levels, the decomposition is done recursively only on the low pass approximation coefficients obtained at the previous level. The process is continued for the required number of levels. However, in the case of WPD, both the detail and approximation coefficients are decomposed at each level. An illustration of WPD is given in Fig. 4. A1 depicts the approximation coefficients obtained at level 1 of decomposition and D1 the detail coefficients. Similarly, AA2 and DA2 are the approximation and detail coefficients obtained at level 2 by decomposing A1. These coefficients can be used as features that describe the epileptic activities.
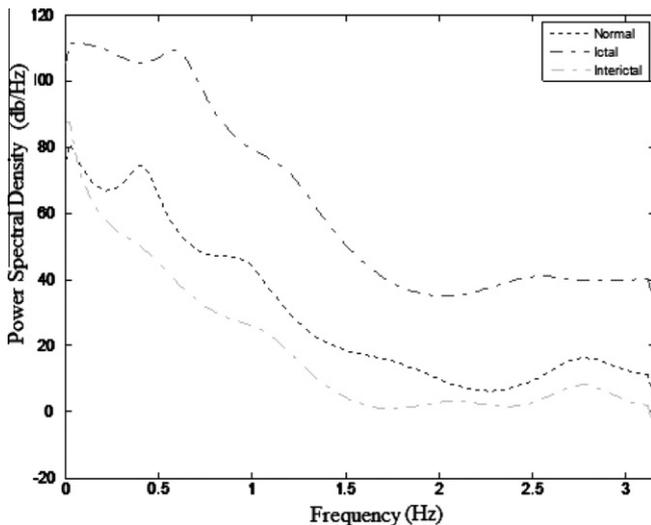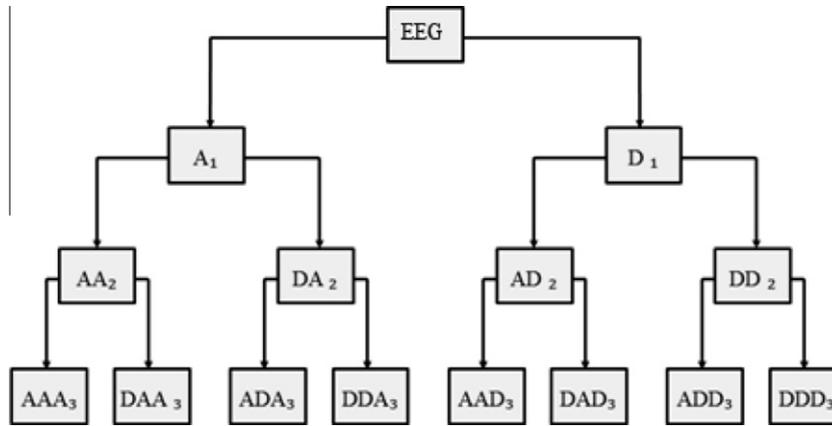
Fig. 4. Wavelet packet decomposition.

2.1.3.2. Hilbert–Huang Transform (HHT). The Hilbert–Huang Transform (HHT) is used to decompose a signal into Intrinsic Mode Functions (IMFs) in order to obtain instantaneous frequency data. In the context of epilepsy detection, Empirical Mode Decomposition (EMD) is first applied to extract the intrinsic modes in the EEG signal. Subsequently, Hilbert Transform is applied to every intrinsic mode to track instantaneous frequencies and amplitudes. Then Hilbert weighted frequency is determined which is used to discriminate between healthy and seizure activities [78]. Empirical Mode Decomposition (EMD) is a simple, adaptive, nonlinear method which can provide variability in the given time series [46]. EMD yields few IMFs, which are amplitude and frequency modulated (AM and FM) waves. Martis et al. [68] classified normal, interictal and ictal EEG time series using EMD techniques and reported an accuracy of 95.3%. We have shown eight IMFs for normal, interictal and ictal EEG signals in Fig. 5.

2.1.4. Nonlinear method of analysis

Frequency domain methods can capture rhythmic oscillations in a signal, but are limited by the inability to detect nonlinear coupling and phase locking among harmonics in the same spectrum [22]. Biological systems can be represented in an effective way using nonlinear techniques. This is true for EEG signal analysis too. The various useful and tried nonlinear parameters for the detection of epilepsy using EEG signals are HOS, Largest Lyapunov Exponent (LLE), Correlation Dimension (CD), Fractal Dimension (FD), Hurst Exponent (H), entropies like Approximate Entropy (ApEn) and Sample Entropy (SampEn), and Recurrence Quantification Analysis (RQA). In this section, we briefly describe these parameters.

2.1.4.1. Higher Order Spectra (HOS). Higher order spectral analysis is a powerful tool for conducting nonlinear dynamical analysis of nonlinear, non-stationary and non-Gaussian physiological signals. HOS analysis can detect nonlinearity, deviations from Gaussianity and phase relationships between harmonic components of the signal. HOS are used to analyze signals and extract useful features which can be used to detect abnormalities. HOS (also called as polyspectra) is the spectral representation of higher order statistics, i.e. moments and cumulants of third and higher order. It can measure non-Gaussianity and separate non-Gaussian signal from an additive mixture of independent non-Gaussian signals and Gaussian noise using the property that HOS of Gaussian signals are statistically zero. The high noise immunity provided by HOS techniques is specifically useful in cases where the signals are corrupted with Gaussian noise. Another advantage is that HOS can

preserve the true phase character of signals. Most of the work done so far in HOS used the third order statistics named bispectrum $B(f_1, f_2)$ which is the third order cumulant generating function. It can also be defined as the FT of the third order correlation of a signal. It is given by

$$B(f_1 f_2) = E[X(f_1)X(f_2)X(f_1 + f_2)] \qquad (7)$$

where $X(f)$ is the FT of the signal $X(nT)$, n is an integer index, T is the sampling interval and $E[\cdot]$ is the expectation operator. The expectation operator can be omitted for deterministic signals. For deterministic sampled signals, $X(f)$ is the discrete-time FT computed using Fast Fourier Transform (FFT). From the equation, it can be seen that bispectrum is a triple product evaluated at two frequencies and their sum frequency. Bispectrum gives the cross correlation between frequency components in a two-dimensional frequency plot. The nonlinear interactions between harmonic components of a signal are thus clearly evident from the bispectrum plot. Bispectrum is a function of two frequencies whereas power spectrum is a function of one frequency variable. Several useful parameters can be extracted from bispectrum. Some of these derived HOS parameters are [3]

(a) Normalized bispectral entropy (P_1):

$$P_1 = \sum_n p_n \log p_n \qquad (8)$$

where

$$p_n = \frac{|B(f_1, f_2)|}{\sum_\Omega |B(f_1, f_2)|} \qquad (9)$$

(b) Normalized bispectral squared entropy (P_2):

$$P_2 = -\sum_n q_n \log q_n \qquad (10)$$

where $q_n = \frac{|B(f_1, f_2)|^2}{\sum_\Omega |B(f_1, f_2)|^2}$ and Ω is the region where $f_1 > f_2$ and $f_1 + f_2 < 1$ as shown in Fig. 6. This region is termed as the principal domain or the non-redundant region for the computation of bispectrum of real signals.

(c) Mean bispectrum magnitude is

$$M_{ave} = \frac{1}{L} \sum_\Omega |B(f_1, f_2)| \qquad (11)$$

Here L is the number of points within the region in Fig. 6.

(d) The bispectrum phase entropy (P_e)
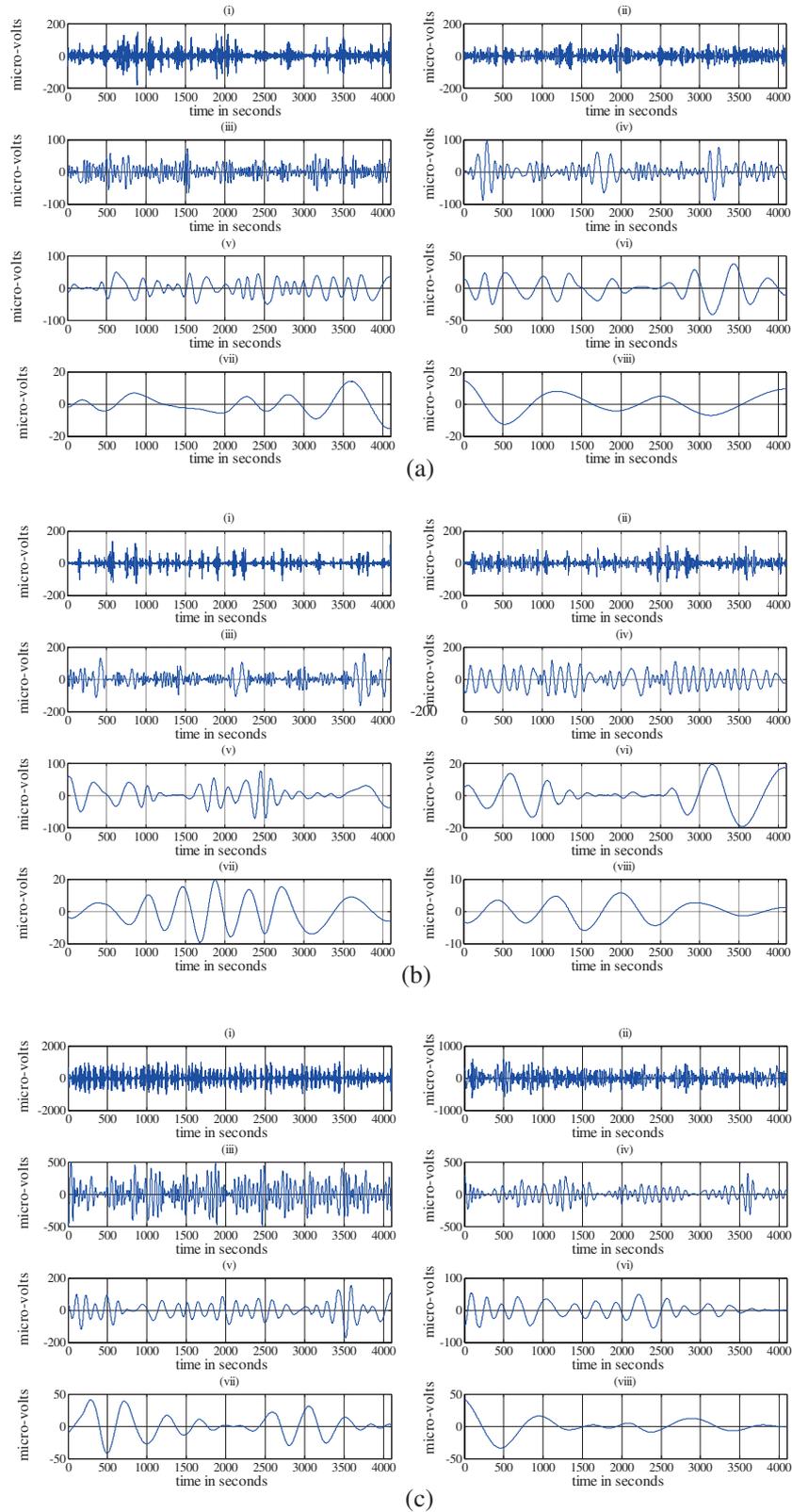
Fig. 5. Typical plots of IMFs derived from EMD decomposition (a) normal, (b) interictal and (c) ictal EEG signals shown in Fig. 1.

$$P_e = \sum_n p(\Psi_n) \log \Psi_n \qquad (12)$$

where

$$p(\Psi_n) = \frac{1}{L} \sum_\Omega 1(\Phi(b(f_1,f_2))\Psi_n) \qquad (13)$$

where

$$\Psi_n = \left\{ \Phi/ -\pi + 2\pi n/N \leqslant \Phi < -\pi + \frac{2\pi(n+1)}{N}, \quad n = 0,1,..N-1 \right. \qquad (14)$$

Φ is the phase angle of bispectrum and $1(\cdot)$ is the indicator function which has the value 1 when phase angle Φ lies within the range of
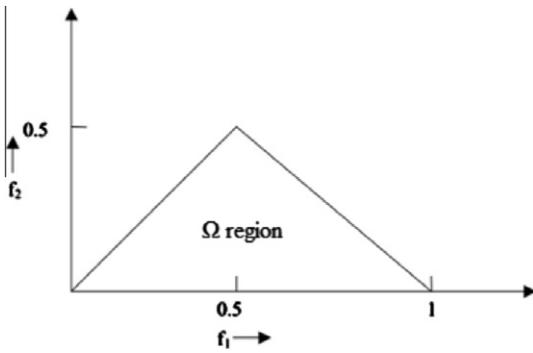
Fig. 6. Non-redundant region of computation of bispectrum (frequencies shown are normalized by Nyquist frequency).

bin Ψ_n in Eq. (14). The phase entropy parameter increases with the increase of randomness of the process.

Chua et al. [23] and Acharya et al. [3] used HOS parameters for the automated detection of epilepsy. Fig. 7 shows the bispectrum (left) and its contour plot (normalized derivative of bispectrum) (right) for normal (a), interictal (b) and ictal (c) segments shown in Fig. 1. Fig. 8 shows the bicoherence (left) and its contour plot (normalized derivative of bispectrum) (right) for normal (a), interictal (b) and ictal (c) segments shown in Fig. 1. Table 1 shows the values of P_1, P_2, and P_e for the signals in Fig. 1. The difference of these HOS features among the three segments is clearly evident from both the figure and table.

2.1.4.2. Higher order cumulants. It is very difficult to evaluate the nonlinear dynamic property of the bio-signals using first and second order statistics [73]. Hence, third order cumulant which highlights the nonlinear behavior can be used for EEG signals. Cumulants are a class of HOS features widely used in many applications for EEG analysis [126,117]. Acharya et al. [3] also used cumulants for the automated detection of epilepsy.

Suppose $\{x_1, x_2, x_3, \ldots, x_k\}$ denote a k dimensional multivariate zero mean random process. The first four order moments are [73],

$$m_1^x = E[x(n)] \tag{15}$$
$$m_2^x(i) = E[x(n)x(n+i)] \tag{16}$$
$$m_3^x(i,j) = E[x(n)x(n+i)x(n+j)] \tag{17}$$
$$m_4^x(i,j,k) = E[x(n)x(n+i)x(n+j)x(n+k)] \tag{18}$$

where m_1^x, m_2^x, m_3^x and m_4^x are the first four order moments, $E[\cdot]$ is the expectation operator, i and j are the time lag parameters. The cumulants can be computed as nonlinear combinations of moments [73] and is given by

$$C_1^x = m_1^x \tag{19}$$
$$C_2^x = m_2^x(i) \tag{20}$$
$$C_3^x = m_3^x(i,j) \tag{21}$$

$$C_4^x = m_4^x(i,j,k) - m_2^x(i) - m_2^x(j-k) - m_2^x(k-i) - m_2^x(k)m_2^x(i-j) \tag{22}$$

where C_1^x, C_2^x, C_3^x and C_4^x are the first four order cumulants respectively. In this work, third order cumulant is used for the analysis of EEG signals. Fig. 9 shows the third order cumulant plots and its contour plot for typical normal, interictal and ictal EEG signal shown in Fig. 1.

2.1.4.3. Recurrence Plot (RP) and Recurrence Quantification Analysis (RQA).
2.1.4.3.1. Recurrence Plot (RP). Recurrence plot, proposed by Eckmann [27] is a two-dimensional graphical plot, which displays the recurrences of states. RP can find out hidden periodicities in a signal in time domain which are not easily noticeable. It can measure the non-stationarity of a time-series signal. Recurrence is said to

have occurred when the distance between two states i and j falls below a threshold value ε. Let x_i be the ith point on the orbit in an m-dimensional space. Whenever x_j is sufficiently close to x_i, a dot is placed at (i, j). The plots are symmetric along the diagonal $i = j$ because if x_i is close to x_j, then x_j is close to x_i. Thus, recurrence plot is an array of dots in an $N \times N$ square. It can also be viewed as an $N \times N$ matrix of black and white dots in time related space. Here black dot means recurrence has occurred. Acharya et al. [4] used RP for identifying normal, interictal, and ictal EEG signals. Fig. 10 shows the RPs of normal, interictal and ictal EEG signals of Fig. 1 (taking 1000 samples). It can be observed that RPs are unique for each class and rhythmicity increases gradually from Fig. 10a–c.

2.1.4.3.2. Recurrence Quantification Analysis (RQA). RQA measures the number and duration of recurrences in a dynamical system. It is used to quantify the Recurrence plot of EEG signal. RQA measures the non-stationarity and hidden periodicities in a time domain signal. For the non-stationary input data signal, RQA gives parameters which are measures of complexity and nonlinearity. Webber and Zbilut [121], Zbilut and Webber [127] and Marwan et al. [69] were the main developers of RQA techniques. Acharya et al. [4] used RQA features for the three-class classification of EEG signals for detecting epilepsy. The RQA features used are as follows:

(a) *Mean diagonal line length $\langle L \rangle$ or L_{mean}:* $\langle L \rangle$ is an indicator of the mean prediction time of the system. The inverse of divergence of the system is measured by this parameter. It is defined as

$$L_{mean} = \frac{\sum_{l=l_{min}}^{N} lP(l)}{\sum_{l=l_{min}}^{N} P(l)}. \tag{23}$$

(b) *Longest diagonal line (L_{max}):* L_{max} is length of the longest diagonal line in the RP. It is defined as $L_{max} = \max(\{l_i; i = 1, \ldots, N_l\})$. Here N_l represents the number of diagonal lines in the recurrence plot.

(c) *Longest vertical line V_{max}:* V_{max} is length of the longest vertical line in RP. It is defined as $V_{max} = \max(\{v_i; i = 1, \ldots, N_v\})$.

(d) *Recurrence Rate (REC):* REC indicates the density of recurrence points present in a recurrent plot. As described earlier, a black dot indicates that recurrence has occurred. REC is defined as

$$REC = \frac{1}{N^2} \sum_{i,j=1}^{N} R_{i,j} \tag{24}$$

where $R_{i,j}$ is the representation of recurrence plot, N is the number of points $R_{i,j}$ on the phase space trajectory; it represents the total number of states considered.

(e) *Determinism (DET):* DET is the fraction of recurrence points which form the diagonal line in the RP and is defined as

$$DET = \frac{\sum_{l=l_{min}}^{N} lP(l)}{\sum_{i,j=1}^{N} R(i,j)} \tag{25}$$

Here $P(l)$ is the frequency distribution of the lengths l of the diagonal lines (proportion of diagonal lines of length l over the total diagonal lines). l_{min} is the length of the minimum diagonal line. DET measures the predictability and determinism of the system.

(f) *Entropy (ENTR):* The complexity of the recurrence system is given by entropy. It is a measure of the average information contained in the line-segment distribution. It is given by

$$ENTR = - \sum_{\ell=\ell_{min}}^{N} p(\ell) \ln p(\ell) \tag{26}$$
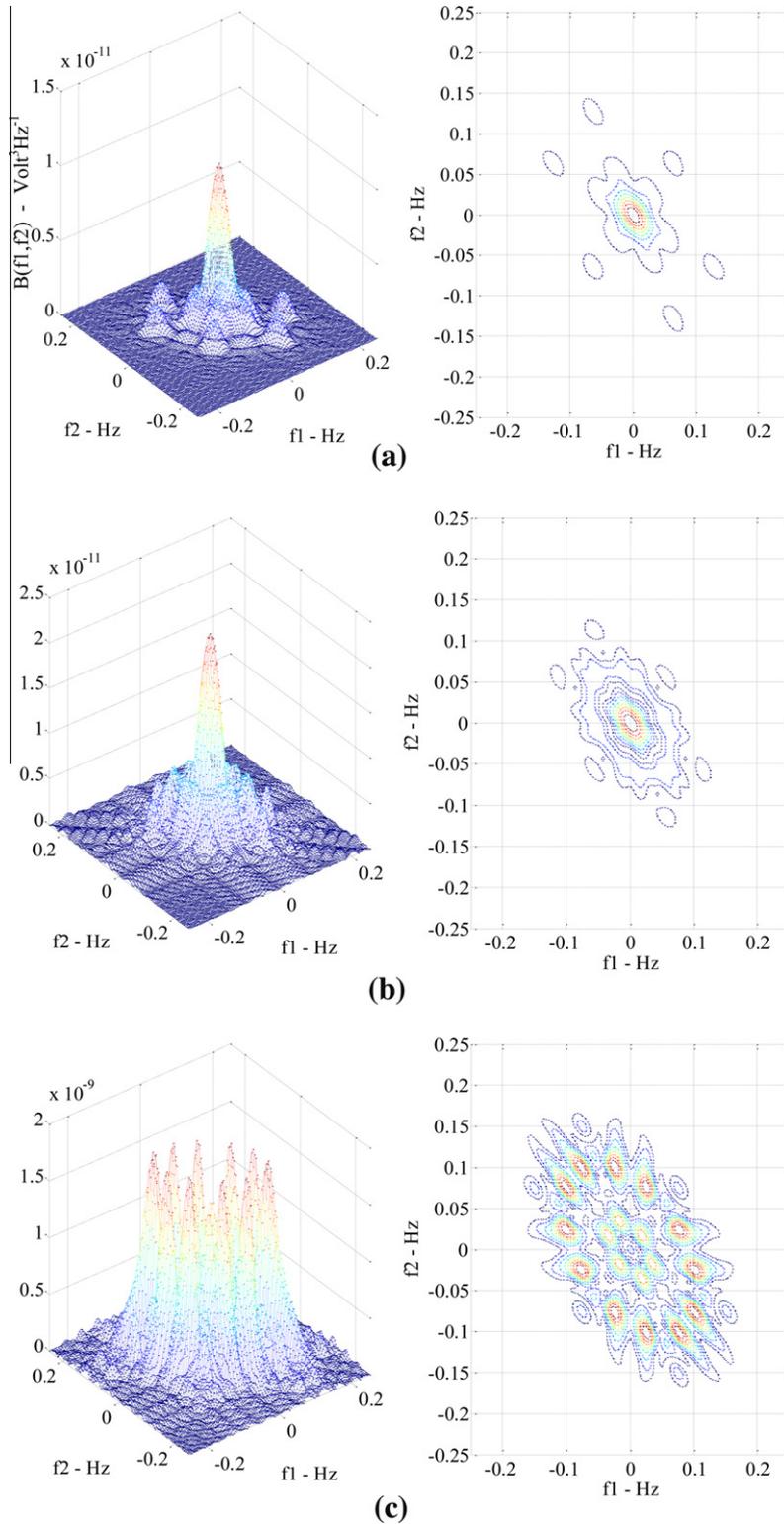
Fig. 7. Plots of bispectrum (left) and its contour (right) for (a) normal (b) interictal (c) ictal signals shown in Fig. 1.

(g) *Laminarity (LAM)*: LAM is the fraction of recurrence points which form the vertical lines. It is an indicator of the number of laminar states in the system.

$$LAM = \frac{\sum_{v=v_{min}}^{N} vP(v)}{\sum_{i,j=1}^{N} P(v)} \qquad (27)$$

Here $P(v)$ is histogram of the length v of the vertical lines.

(h) *Trapping time (TT)*: This is related to the average length of the vertical lines. It is the average time the system remains in one state or changes its state very slowly.

(i) *Recurrence time* of the recurrence plots is calculated as $T(i) = t_{i+1} - t_i$ where $t = 1, 2, \ldots, K$.
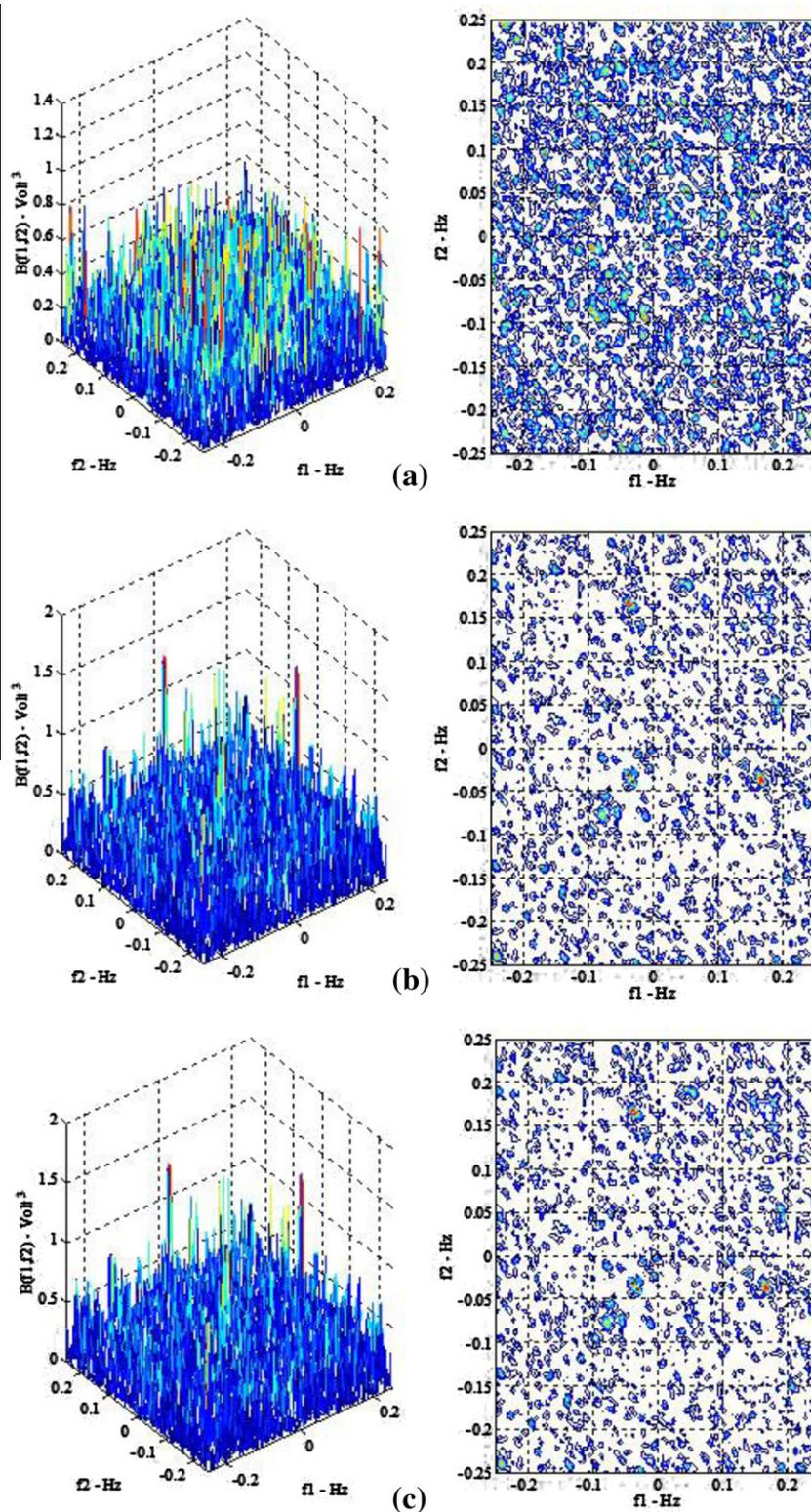
Fig. 8. Plots of bicoherence (left) and its contour (right) for (a) normal, (b) interictal and (c) ictal signals shown in Fig. 1.

Table 2 shows the results of RQA parameters for normal, inter-ictal and ictal EEG signals shown in Fig. 1. It is evident that the RQA parameters are different for the three classes.

2.1.4.4. Approximate Entropy (ApEn). ApEn was proposed by Pincus [84] and it is a measure of regularity of data. The value of *ApEn* is more for more complex or irregular data. An irregular time series results in a higher non-negative value for *ApEn* while a regular

and predictable time series signal results in low *ApEn* value [85]. Let R^m be the embedding space and $x(1), x(2), \ldots, x(N)$ be the N data points, then *ApEn* is calculated as

$$ApEn(m, r, N) = \frac{1}{N-m+1} \sum_{i=1}^{N-m+1} \log C_i^m(r) - \frac{1}{N-m} \sum_{i=1}^{N-m} \log C_i^{m+1}(r)$$

(28)

Table 1
Results of normalized bispectrum entropy1 (P_1), normalized bispectrum entropy2 (P_2), and phase entropy (P_e) for normal, interictal and ictal EEG signals shown in Fig. 1.

Features	Normal	Interictal	Ictal
P_1	0.665	0.510	0.688
P_2	0.421	0.207	0.512
P_e	3.578	3.569	3.395

where

$$C_i^m = \frac{2}{N_m(N_m-1)} \sum_{i=1}^{N_m} \sum_{j=1, j\neq i}^{N_m} \Theta(r - \|x_i - x_j\|) \tag{29}$$

Kannathal et al. [59] and Acharya et al. [6] used *ApEn* for discriminating epileptic stages. Table 3 shows the *ApEn* values for the normal, interictal, and ictal EEG signals shown in Fig. 1.

(a)

(b)

(c)
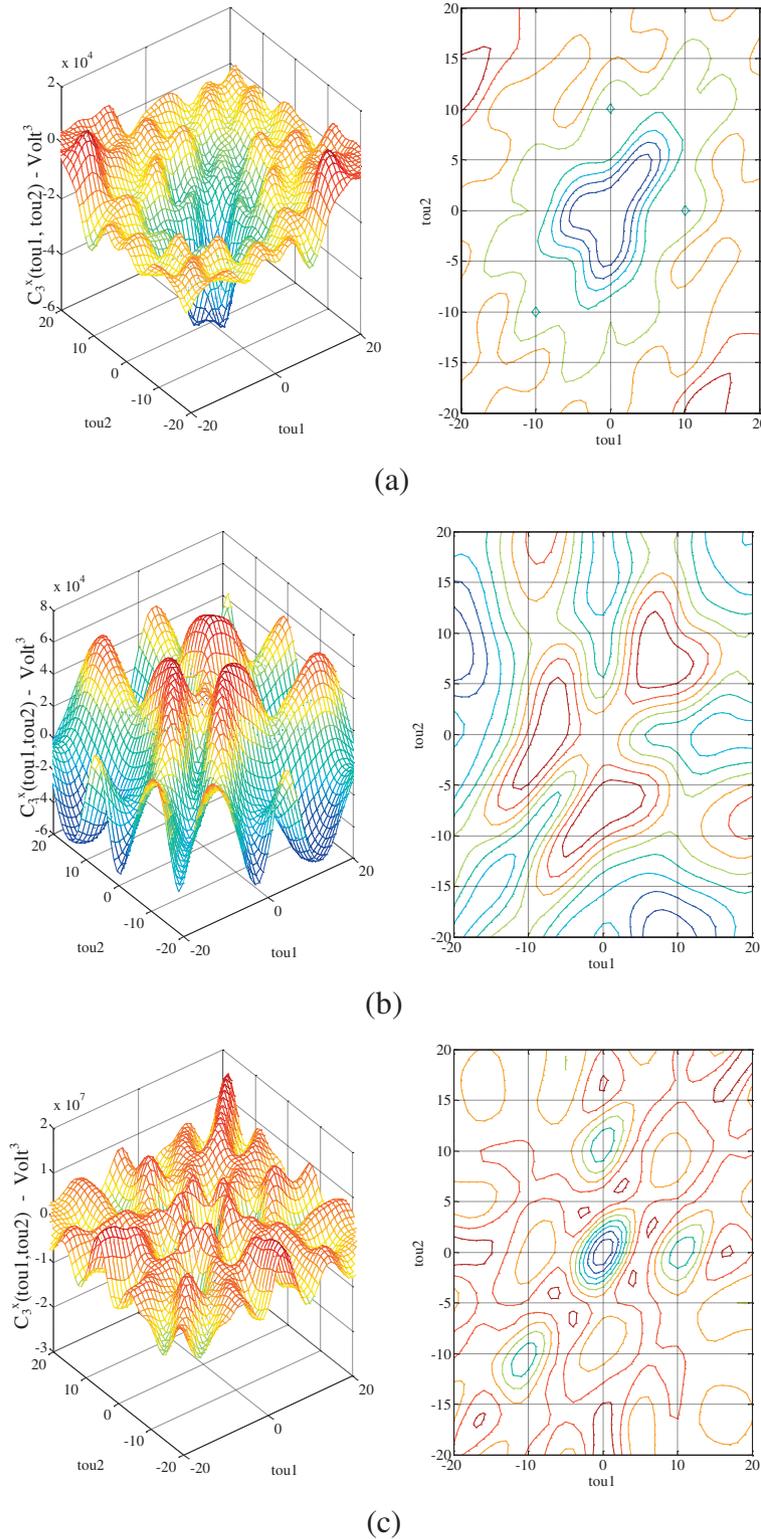
Fig. 9. Plots of 3rd order cumulent (left) and its contour (right) for (a) normal, (b) interictal and (c) ictal signals shown in Fig. 1.
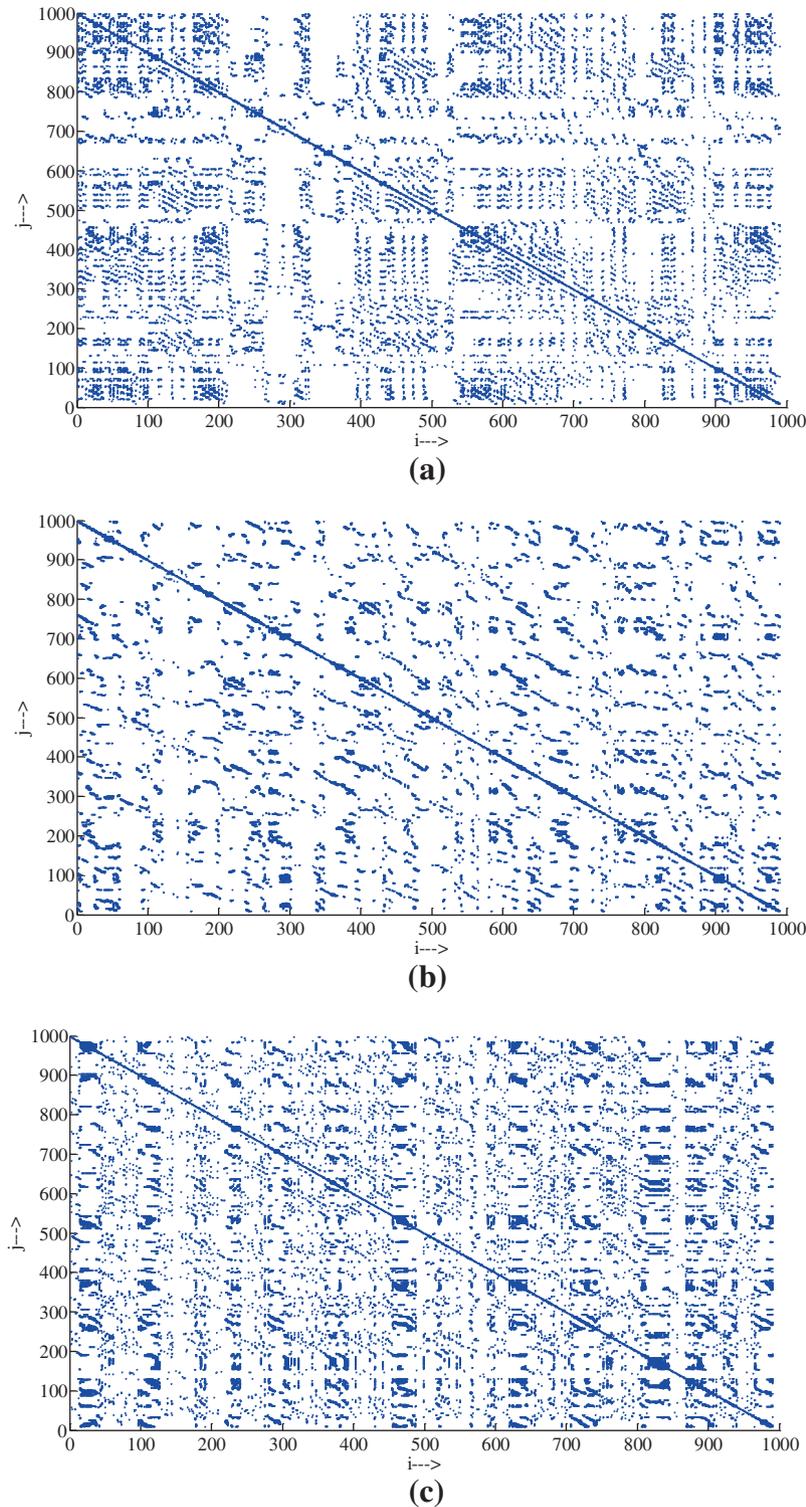
Fig. 10. Results of recurrence plots of (a) normal, (b) interictal and (c) ictal EEG signals shown in Fig. 1.

2.1.4.5. Sample Entropy (SampEn). Richman and Randall [96] developed the parameter called *SampEn* and it also measures the complexity and regularity of the time-series data. *SampEn* is also a measure of self-similarity. Lower *SampEn* value implies high self-similarity, and higher values are registered for more irregular data. *SampEn* is an improved measure when compared to *ApEn*. Epilepsy causes a reduction in both these entropy parameters. Table 4 shows the *SampEn* values for the normal, interictal, and ictal EEG signals shown in Fig. 1.

2.1.4.6. Fractal Dimension (FD). Mandelbrot [66] introduced the term 'fractal'. The concept of fractal dimension originates from fractal geometry. FD is a powerful tool for transient detection. It can be used to measure the dimensional complexity of biological signals. It can give an indication of how completely the fractal appears to fill space. A fractal is a geometric shape which can be divided into smaller components. Each of these components represents a reduced copy of the original from which it is derived. FD can be calculated from a set of points using several methods

Table 2
Results of RQA parameters for normal, interictal and ictal EEG signals shown in Fig. 1.

Features	Normal	Interictal	Ictal
RR	0.052	0.060	0.087
DET	0.266	0.496	0.518
$\langle L \rangle$	2.279	2.503	3.169
$L_{\max}$	8	10	38
ENTR	0.669	0.956	1.471
LAM	0.353	0.630	0.684
TT	2.425	2.783	3.878
$V_{\max}$	7	11	20
T1	19.051	16.498	11.449
T2	24.055	27.711	23.315

that differ in accuracy, sensitivity to the number of points used and the time required for computation (Estellar et al. [28] and Kallimanis et al. [58]). The algorithm proposed by Higuchi is generally used for finding FD of EEG signals. Higuchi [44] introduced the algorithm as an effective technique to analyze non-periodic and irregular time series better and achieve precise and stable FD. The EEG signal is assumed as the time sequence $x(1), x(2), \ldots, x(n)$. Time series x_m^k may be constructed as:

$$x_m^k = \left\{ x(m), x(m+k), x(m+2k), \ldots, x\left(m + \left[\frac{N-m}{k}\right]k\right) \right\} \quad (30)$$

where $m = 1, 2, \ldots, k$. Here m indicates the initial time value and k indicates the discrete time interval between points. The length $L_m(k)$ for each of the k time series or curves x_m^k is computed as:

$$L_m(k) = \frac{\sum_{i=1}^{\lfloor a \rfloor} |x(m+ik) - x(m+(i-1)k)|(N-1)}{\lfloor a \rfloor k} \quad (31)$$

where n is the total length of data sequence x. The mean value of the curve length $L_m(k)$ is calculated for each k by averaging $L_m(k)$ for all m. Thus, an array of mean values $L_m(k)$ is obtained. A plot of $\log(L_m(k))$ versus $\log\left(\frac{1}{k}\right)$ is made and FD is estimated from the slope of least squares linear best fit from the plot. In other words, FD can be defined as FD $= \log(L_m(k))/\log(1/k)$ [44]. Table 5 shows the FD values for normal, interictal, and ictal EEG signals shown in Fig. 1.

2.1.4.7. Correlation Dimension (CD). Correlation Dimension (CD) is a nonlinear parameter which can be used as a useful indicator of pathologies. CD is a widely used measure of fractal dimension. The widely used algorithm for calculating CD is the Grassberger–Procaccia algorithm proposed by Grassberger and Procassia [38]. As per this algorithm, a function $C(r)$, which is the probability that two arbitrary points on the orbit are closer together than r, is constructed. The correlation function $C(r)$ is calculated as follows

$$C(r) = \frac{1}{N^2} \sum_{x=1}^{N} \sum_{y=1, x \neq y}^{N} \Theta(r - |X_x - X_y|) \quad (32)$$

Here X_x and X_y are points of the trajectory in the phase space, N is the number of data points in phase space, r is the radial distance around each reference point and Θ is the Heaviside function. CD is then calculated using the equation:

$$CD = \lim_{r \to 0} \frac{\log C(r)}{\log(r)} \quad (33)$$

Table 6 shows the CD values for normal, interictal, and ictal EEG signals shown in Fig. 1.

Table 3
ApEn values for normal, interictal, and ictal EEG signals shown in Fig. 1.

Features	Normal	Interictal	Ictal
ApEn	2.216	1.781	1.885

Table 4
SampEn values for normal, interictal, and ictal EEG signals shown in Fig. 1.

Features	Normal	Interictal	Ictal
SampEn	1.301	1.048	0.796

2.1.4.8. Hurst Exponent (H). Hurst exponent is a measure of self-similarity, predictability and the degree of long-range dependence in a time-series. It is also a measure of the smoothness of a fractal time-series based on asymptotic behavior of the rescaled range of the process [30,91]. According to the Hurst's generalized equation [48] of time series, Hurst exponent H is defined as

$$H = \frac{\log(R/S)}{\log(T)} \quad (34)$$

where T is the duration of the sample of data and R/S is the corresponding value of rescaled range. R is the difference between the maximum and minimum deviation from the mean while S represents the standard deviation [25]. Hurst exponent is estimated by plotting (R/S) versus T in log–log axes. The slope of the regression line approximates the Hurst exponent. Table 7 shows the H values for normal, interictal, and ictal EEG signals shown in Fig. 1.

2.1.4.9. Largest Lyapunov Exponent (LLE). Largest Lyapunov exponent is a measure of the dependence of the system on initial conditions. It defines the average rate by which two neighboring trajectories diverge or separate from one another. A negative exponent indicates that orbits approach a common fixed point, while a zero exponent means that orbits maintain their relative positions. If a positive *LLE* is achieved, it indicates the existence of chaos in that system. An algorithm for calculating *LLE* was proposed by Wolf et al. [123]. Another method for calculation was devised by Rosenstein et al. [98] which was used in this study. It works on recorded time-series uses the nearest neighbor of each point in phase-space and traces their separation over certain time development. The *LLE* is then calculated by means of a least squares fit to the "average" line defined by:

$$y(i) = \frac{1}{\Delta t} \langle \ln d_j(i) \rangle \quad (35)$$

Here $d_j(i)$ represents the distance between each phase space point and its nearest neighbor at time ith step, and $\langle \cdot \rangle$ denotes the average overall phase space points. Table 8 shows the LLE values for normal, interictal, and ictal EEG signals shown in Fig. 1.

2.2. Surrogate data analysis

Surrogate data analysis is performed to test whether there is nonlinearity in the original data [113]. The original data is subjected to phase randomization to obtain the surrogate data. The surrogate data sequence has the same mean, variance, autocorrelation, and power spectrum as the original data sequence. But the phase relationships present in the original data will be completely lost in the surrogate data sequence. The random phase spectrum of the derived surrogate data can be achieved by any of the three methods of random phase, phase shuffle and data shuffle [59]. For the EEG analysis, nonlinear parameters like CD, LLE are computed for several surrogate data series and they are compared with

Table 5
FD values for normal, interictal, and ictal EEG signals shown in Fig. 1.

Features	Normal	Interictal	Ictal
FD	−1.413	−1.345	−1.461

Table 6
CD values for normal, interictal, and ictal EEG signals shown in Fig. 1.

Features	Normal	Interictal	Ictal
CD	5.39	8.59	2.82

Table 7
H values for normal, interictal, and ictal EEG signals shown in Fig. 1.

Features	Normal	Interictal	Ictal
H	0.7194	0.8727	0.5546

Table 8
LLE values for normal, interictal, and ictal EEG signals shown in Fig. 1.

Features	Normal	Interictal	Ictal
LLE	3.8501	2.9444	6.7946

those computed using the original data series. If there is significant difference (more than 50%) in the nonlinear parameter values between those obtained from original and surrogate data, it is a strong indication of nonlinearity in the original EEG signal [2].

2.3. Necessity of nonlinear methods for EEG analysis

EEG signals have significant nonlinearity [107]. EEG signals are generated mainly by the firing of post-synaptic neurons when their membrane exceeds a certain threshold. An EEG signal is comprised of several sinusoidal components of distinct frequencies. These components have nonlinear interactions among themselves producing more sinusoidal components at sum or difference frequencies [128]. Any method which can detect the nonlinear behavior of EEG signals can provide much better information about the state of central nervous system and brain [101]. The nonlinear dynamical theory has its basis on the concept of chaos and it is widely used in many applications including medicine and biology. Experiments over the past 30 years have shown that chaotic systems are common in nature. Boccaletti et al. [18] describe a chaotic system in detail. Glass et al. [37], Jeong et al. [55], and Philippe and Henri [81] found that schizophrenia, insomnia, epilepsy and other disorders can be identified by studying the chaotic behavior of the neurons. Babloyantz et al. [14], Pritchard and Duke [90], and Rey and Guillemant [95] employed nonlinear techniques for analyzing sleep signals and EEG waveform. Rapp et al. [93] and Rapp [94] explained neural processes and brain signals using nonlinear dynamics and chaos. Literature [108,45] shows that nonlinear methods are used for the analysis of several physiological signals related to heart and respiratory dynamics. Nonlinear dynamical analysis methods have been widely employed for extracting maximum information from EEG signals [10,11,62,111] and for improving the reliability of the results of analysis. Lehnertz and Elger [64] found that time-resolved analysis of the EEG signals recorded from within the seizure-generating area of the brain showed changes in the nonlinear characteristics for up to several minutes prior to seizures. Martinerie et al. [67] conducted a dimension analysis of EEG and reached the conclusion that epileptic seizures are states with reduced dimensionality compared to normal epileptic states, and hence, showed the possibility of prediction of seizures. Lehnertz and Elger [63] studied about the relationships between neurons and epileptic region by analyzing the spatial extent and temporal dynamics using correlation dimension techniques. Pijn [82] and Pijn et al. [83] conducted the quantitative evaluation of epilepsy with intracranial EEG signals as input by using the techniques of

nonlinear dynamics. Jing and Takigawa [56] used correlation dimension techniques to study the different neurological states of epilepsy using EEG signal. Andrzejak et al. [10] used a new measure ξ to discriminate between nonlinear deterministic and linear stochastic systems. It was found that EEG signals recorded from epileptic regions displayed strong nonlinear determinism while non-epileptic zones can be characterized as linear stochastic systems. Aschenbrenner-Scheibe et al. [12] proposed several methods for the detection of onset of seizures based on EEG recordings and analysis of a nonlinear feature motivated by correlation dimension. They studied the dimension drop in the pre-ictal state. Paivinen et al. [79] used nonlinear features and computational methods like discriminant analysis to analyze EEG and to detect epileptic seizures in addition to time and frequency domain methods. Bai et al. [15] used nonlinear parameters like sample entropy for analyzing epileptic EEG signals and observed that epilepsy resulted in a reduction of sample entropy and approximate entropy values. Freeman [32] and Wright and Liley [125] proposed EEG models for the domain of neurobiology. Theiler [112], Theiler et al. [113], Rombouts et al. [97], Lamberts et al. [62], and Bradley [19] used nonlinear measures for analyzing EEG data. Nonlinear characteristics of EEG were studied to test the differences between groups of healthy and diseased people [16,70,54] and to identify different sleep stages [31]. All these studies emphasize the importance of nonlinear method of analysis of EEG signals to understand and study its nature in various brain related disorders, and therefore, such analysis is apt for detection of epileptic stages.

3. Epilepsy activity classification

All the studies summarized in this section used the Bonn University dataset [10]. This dataset includes five subsets (denoted as Z, O, N, F and S), each containing 100 single-channel EEG segments of 23.6 s duration. All the segments were recorded using a 128-channel amplifier system, digitized with a sampling rate of 173.61 Hz and 12-bit A/D resolution, and filtered using a 0.53–40 Hz (12 dB/octave) band pass filter. The normal segments (Sets Z and O) were taken from the five healthy subjects. The standard surface electrode placement scheme (the international 10–20 system) was used to obtain the EEG from the healthy cases. Volunteers were relaxed in an awake state with eyes open (Z) and eyes closed (O), respectively. Both the interictal and ictal segments were obtained from five epilepsy patients. The interictal segments were recorded during seizure free intervals from the depth electrodes that were implanted into the hippocampal formations (Set N) and from the epileptogenic zone (Set F). The ictal segments (Set S) were recorded from all sites exhibiting ictal activity using depth electrodes and also from strip electrodes that were implanted into the lateral and basal regions of the neocortex [10].

3.1. Studies that presented techniques for two-class (normal, ictal) epilepsy activity classification

Nigam and Graupe [71] used a multistage nonlinear pre-processing filter along with an Artificial Neural Network (ANN) for the automated detection of epileptic signals and obtained an accuracy of around 97.20%. Nonlinear parameters like CD, LLE, H, and entropy were used to characterize the EEG signal and discriminate epileptic and alcoholic EEG from normal EEG with more than 90% accuracy [60]. Using the same dataset, the same group automatically classified EEG signals into normal and epileptic using different entropies using an Adaptive Neuro-Fuzzy Interference System (ANFIS) and obtained an accuracy of 92.22% [59]. Time domain and frequency domain EEG features combined with Elman network was used to classify the two classes with an accuracy, sensitivity,

Table 9
Summary of previous works for automated detection of normal and epileptic classes.

Authors	Features	Classifier	Accuracy (%)
Nigam and Graupe [71]	Nonlinear pre-processing filter	Diagnostic neural network	97.20
Kannathal et al. [59]	Entropy measures	Adaptive Neuro-Fuzzy Inference system (ANFIS)	92.22
Srinivasan et al. [103]	Time & frequency domain features	Elman network	99.60
Sadati et al. [99]	DWT	Adaptive neural fuzzy network	85.90
Subasi [109]	DWT-Statistical measures	Mixture expert model (a modular neural network)	94.50
Polat and Gunes [86]	FFT based features	Decision tree	98.72
Tzallas et al. [114]	Time–frequency methods	Artificial neural network	97.72–100
Srinivasan et al. [104]	*ApEn*	Probabilistic neural network, Elman network	100
Polat and Gunes [87]	FFT based features	Artificial immune recognition system	100
Polat and Gunes 88	AR	C4.5 decision tree classifier	99.32
Ocak [74]	DWT-*ApEn*	Thresholding	96.65
Guo et al. [40]	Relative Wavelet Energy	ANN	95.20
Guo et al. [41]	ApEn and Wavelet Transform	ANN	99.85
Guo et al. [42]	Line length features and Wavelet Transform	ANN	99.60
Subasi and Gursoy [110]	DWT-PCA, ICA, LDA	SVM	98.75(PCA) 99.50(ICA) 100(LDA)
Ubeyli [116]	AR	SVM	99.56
Lima et al. [65]	Wavelet Transform	SVM	100
Guo et al. [43]	Genetic programming based	KNN	99
Wang et al. [120]	Wavelet packet entropy	KNN	100
Iscan et al. [53]	Cross correlation and PSD	Several classifiers including SVM	100
Orhan et al. [75]	DWT	ANN	100

and specificity of 99.6% [103]. Normal and epileptic EEG signals were automatically identified with a classification accuracy of 85.9% using DWT sub-band energy as input features to adaptive neural fuzzy network [99].

Srinivasan et al. [104] developed an automated epileptic EEG detection system using approximate entropy as the feature in Elman and probabilistic neural networks. Elman network yielded an overall accuracy of 100%. Tzallas et al. [114] employed time–frequency methods to analyze selected segments of EEG signals for automated detection of seizure using neural network and obtained an accuracy ranging from 97.72% to 100%. Subasi [109] applied DWT on EEG signals and decomposed them into frequency sub-bands. DWT coefficients were converted into four statistical features and these were fed to a modular neural network called Mixture of Experts (MEs). They classified normal and epileptic EEG signals with an accuracy of 94.5%, sensitivity of 95%, and specificity of 94%. Polat and Gunes [86] classified EEG signals into epileptic and normal using FFT based Welch method and decision tree classifier and achieved a maximum classification accuracy of 98.72%, sensitivity of 99.4%, and specificity of 99.31%. The same group [87] used the Welch FFT method for feature extraction, PCA for dimensionality reduction, and a new hybrid automated identification system based on artificial immune recognition system (AIRS) with fuzzy resource allocation mechanism for classification of normal and epileptic segments. They reported an accuracy of 100%. The same group ([88] used AR for feature extraction and C4.5 decision tree classifier for classification and reported an accuracy of 99.32%.

Ocak [74] developed a method for automated seizure detection based on *ApEn* and DWT. They were able to distinguish seizures with more than 96% accuracy. Guo et al.'s group conducted many studies using ANN for classification and reported an accuracy of 95.2%, sensitivity of 98.17%, and specificity of 92.12% using relative wavelet energy based features [40], an accuracy of 99.85%, sensitivity of 100%, and specificity of 99.2% using wavelet transform and ApEn features [41], an accuracy of 99.60% using wavelet transform and line length feature [42], and an accuracy of 99% using genetic programming based features in a K-Nearest Neighbor (KNN) classifier [43]. The DWT features were reduced using PCA, ICA and LDA and the resultant features were used to classify normal and epilepsy EEG signals using Support Vector Machine (SVM) classifier

[110]. They obtained an accuracy of 98.85% using PCA method, 99.5% using ICA method and 100% using LDA method. Ubeyli [116] used AR methods for feature extraction and SVM for classification and reported an accuracy of 99.56%. In other recent studies, 100% classification accuracy was achieved by Lima et al. [65] (wavelet transform and SVM), Wang et al. [120] (wavelet packet entropy and KNN), Iscan et al. [53] (cross correlation and PSD and SVM), and Orhan et al. [75] (DWT and ANN).

Table 9 gives a summary of the above listed studies for automated detection of normal and epileptic classes. It can be observed that a variety of methods like FFT, time–frequency, DWT, statistical measures, nonlinear, chaotic and entropy measures, dimension reduction methods like PCA, ICA and LDA are used to analyze EEG to detect epileptic state from normal state. Among these methods, nonlinear methods and time–frequency related techniques, specifically DWT based methods, resulted in higher accuracies.

3.2. Studies that presented techniques for three-class (normal, interictal, ictal stages) epilepsy activity classification

Aslan et al. [13] studied epilepsy groups such as partial and primary generalized epilepsy using a Radial Basis Function Neural Network (RBFNN) and a Multilayer Perceptron Neural Network (MLPNN) and achieved a classification accuracy of 95.2% and 89.2%, respectively. Several studies have been reported which use linear and nonlinear features for the automatic detection of the three EEG classes. Table 10 shows the summary of the features used and the classification accuracies obtained in these studies.

Guler et al. [39] used LLE as a feature in a feed-forward neural network and Recurrent Neural Network (RNN) for the three-class problem. RNN presented an accuracy of more than 96%, sensitivity of around 96%, and specificity of 97.38%. In a recent study [33], wavelets were used to decompose the EEG signals into delta, theta, alpha, beta, and gamma sub-bands. Three features, namely, standard deviation, CD, and LLE were extracted from each sub-band. The authors used a mixed-band feature space consisting of nine parameters in a Spiking Neural Network (SNN) that was trained using three training algorithms (SpikeProp, Quick-Prop and RProp). RProp model resulted in the maximum classification accuracy of

Table 10
Summary of previous works for automated detection of normal, interictal and epileptic classes.

Authors	Features	Classifier	Accuracy (%)
Guler et al. [39]	Lyapunov exponents	Recurrent neural network	96.79
Ghosh-Dastidar and Adeli [33]	Mixed-band feature space	Spiking neural network	92.50
Ghosh-Dastidar et al. [34]	Mixed-band feature space	Back propagation neural network	96.70
Ghosh-Dastidar et al. [35]	Mixed-band feature space	PCA enhanced Cosine radial basis function neural network	96.60
Ghosh-Dastidar and Adeli [36]	Mixed-band feature space	Multi-spiking neural network	90.70–94.80
Chua et al. [22] and Chua et al. [23]	HOS based features	GMM	93.11
Faust et al. [29]	Frequency domain parameters, Burg's method	SVM	93.30
Acharya et al. [2]	Nonlinear features	GMM	95
Guo et al. [43]	Genetic Programming based	KNN	93.50
Orhan et al. [75]	DWT	ANN	96.67
Acharya et al. [3]	HOS cumulants from WPD coefficients	SVM	98.50
Acharya et al. [4]	RQA parameters	SVM	95.60
Acharya et al. [5]	Entropies + HOS + Higuchi FD + Hurst	Fuzzy	99.70
Acharya et al. [6]	Entropies	Fuzzy	98.10
Acharya et al. [7]	PCA eigenvalues from WPD coefficients	GMM	99
Acharya et al. [8]	DWT, ICA coefficients	SVM	96
Martis et al. [68]	Empirical mode	C4.5	95.33

92.5%. In another study by the same group [34], a good classification accuracy of 96.7% was obtained using the Levenberg–Marquardt back propagation neural network and the same nine-parameter mixed-band feature space. The same group [35] developed a novel principal component analysis-enhanced cosine radial basis function neural network classifier to detect epilepsy. Their system yielded a highest accuracy of 96.6%, and was robust to changes in training data with a low standard deviation of 1.4%. During the epilepsy diagnosis, their model yielded an accuracy of 99.3% when only normal and interictal EEGs were considered. Again the same group [36] proposed a multi-spiking neural network wherein information transfer between neurons happens through multiple synapses. They obtained an accuracy range of 90.7–94.8% using the mixed-band feature space to classify the three classes.

Chua et al. [22] applied HOS based features in Gaussian Mixture Model (GMM) and SVM classifiers and obtained an accuracy of 93.11% and 92.67%, respectively. Chua et al. [23] compared HOS features and power spectrum based features and obtained 93.11% classification accuracy for HOS features, while the accuracy was only 88.78% using features derived from power spectrum, both results obtained for the GMM classifier. Faust et al. [29] used three parametric methods for power density spectrum estimation (ARMA, Yule-Walker and Burg's) and evaluated three classifiers. Four local maxima and four local minima parameters were found out (using Billauer's 'peak detection' algorithm: http://billauer.co.il/peakdet.html) [17] from the power density spectrum using Burg's method and given as input to the classifiers. SVM classifier presented the highest classification accuracy of 93.33%, sensitivity of 98.33%, and specificity of 96.67%. Guo et al. [43] and Orhan et al. [75] used the same study protocol used for the two-class problem and obtained lowered accuracies of 93.5% and 96.67%, respectively.

Acharya et al. [2] used four nonlinear parameters namely CD, FD, H and *ApEn* in SVM and GMM classifiers. GMM classifier showed better performance with an average classification accuracy of 95%, sensitivity of 92.22%, and specificity of 100%. In another study by this group [3], HOS cumulants extracted from WPD coefficients were fed to SVM classifier and an accuracy of 98.5%, sensitivity of 100%, and specificity of 100%, was reported. The same group [4] used RQA parameters in an SVM classifier and obtained a classification accuracy of 95.6%, sensitivity of 98.9%, and specificity of 97.8%. In a recent study by this group [5], nonlinear features based on HOS, two entropies, namely *ApEn* and *SampEn*, FD and H were extracted from the EEG segments of 6 s duration. These features in the Fuzzy classifier resulted in 99.7% classification accuracy, and a sensitivity and specificity of 100%. The same group [6]

used *ApEn, SampEn and two phase entropies* in a Fuzzy classifier and reported an accuracy of 98.1%, sensitivity of 99.4%, and specificity of 100%. Again this group recently decomposed EEG segments into wavelet coefficients using WPD, and extracted eigenvalues from the resultant wavelet coefficients using PCA. These features were used in a GMM classifier and accuracy, sensitivity, and specificity of 99% was registered [7]. The same group classified the three classes by applying ICA on the DWT coefficients extracted from various durations of EEG signals (6 s, 12 s, 18 s, and 23.6 s) [8]. They reported the highest classification accuracy of 96%, sensitivity of 96% and specificity of 97% using the SVM classifier for 23.6 s interval data. Spectral peaks, spectral entropy and spectral energy obtained from the waveforms obtained by performing the Hilbert Transform of the intrinsic mode functions were fed to the C4.5 decision tree classifier to classify the three classes [68]. They reported the highest average accuracy of 95.33%, average sensitivity of 98%, and average specificity of 97%.

The results of these studies are further proof to the fact that nonlinear techniques are better applicable for successful EEG analysis, especially for tackling the three-class problem. It is evident from the above summarized studies that the maximum classification accuracy of 100% has been easily achieved in studies that classified normal and epileptic (ictal) stages. However, as highlighted earlier, it is important to determine the interictal or pre-ictal stages to predict the onset of a seizure. For this reason, many studies also focused on classifying normal segments from ictal and interictal segments. From the published literature, it can be seen that the highest accuracy of 99.7% has been achieved for such a three-class classification problem using nonlinear features [5]. Most of these CAD techniques can be written as a software application and easily installed in any physician's office or EEG labs. The process is fully automated as the doctors have to only input the EEG segments, and hence, there is no need for expert training and the results are highly objective.

Even though a technique has been developed for achieving the maximum possible clinically significant accuracy for epilepsy stage classification, there are several areas that have to be addressed before such a technique can be deployed for daily clinical use. First, the current technique has been developed using a benchmark dataset that has been made publicly available for more than a decade now [10]. There is definitely a need to validate the developed technique using several large clinical databases collected using multi-center clinical trials. It is high time that researchers start validating their developed techniques on newly acquired clinical EEG databases rather than trying to improve the classification accuracy which has already reached the highest value possible. Second, studies are needed to determine the accuracy of prediction of the

onset of a subsequent seizure after detecting an interictal/pre-ictal stage. The real use of the availability of an excellent classification technique for the three class problem can only be achieved if it can be extended to predict real-time seizures in patients. Third, one has to address the issue of how good these techniques are in the continuous monitoring of EEG signals for changes in EEG activities. How often should the segments be tested to determine a stage? When should the system alert the user of a possibility of an oncoming seizure? Which electrode setup/arrangement should be in place to record the EEG signals for monitoring?

It may seem like a solution is in place to address the complex problem of subjective visual inspection of tremendous volumes of EEG data. However, there is still a lot of unanswered questions that need to be addressed before such a solution can be implemented for successful clinical use.

4. Conclusions

EEG signals can be used effectively to study the mental states and ailments related to the brain. The inherent issues with the EEG signal are that it is highly nonlinear in nature and its visual interpretations are tedious and subjective prone to inter-observer variations. To help researchers better analyze EEG signals, we have presented various signal analysis techniques such as linear, frequency domain, time–frequency, and nonlinear methods in this review. Our key focus in this review was on epilepsy detection. Epilepsy is a neurological disorder that can cause serious discomfort to the patients due to its abrupt and uncertain nature of presentation. A good side of it is that it is treatable with antiepileptics. An automated system to detect the nature of the seizures at early stage (*interictal*) and to classify normal, interictal, and ictal states can help improving the quality of life by preventing its occurrence. In this regard, we have summarized the findings of many automated epilepsy activity classification techniques that use EEG as the base signal. It is evident from the summary that a combination of the features extracted using the reviewed techniques or sometimes even the features extracted from a single technique can successfully distinguish the three classes. It appears that the use of nonlinear features extracted from EEG segments in classifiers results in high classification accuracies of more than 99%. Even though the highest possible classification accuracy has been achieved for epilepsy activity detection, there are several challenges that have to be faced before such a technique can be clinically used. We have briefly highlighted these challenges and open ended problems that need to be addressed for a fully automated CAD based epilepsy detection and seizure monitoring system to be deployed in a clinical setting.

References

[1] U.R. Acharya, O. Faust, N. Kannathal, T.J. Chua, S. Laxminarayan, Dynamical analysis of EEG signals at various sleep stages, Comput. Methods Programs Biomed. 80 (1) (2005) 37–45.

[2] U.R. Acharya, K.C. Chua, T.C. Lim, Dorithy, J.S. Suri, Automatic identification of epileptic EEG signals using nonlinear parameters, J. Mech. Med. Biol. 9 (4) (2009) 539–553.

[3] U.R. Acharya, S. Vinitha Sree, J.S. Suri, Automatic detection of epileptic EEG signals using higher order cumulant features, Int. J. Neural Syst. 21 (5) (2011) 1–12.

[4] U.R. Acharya, S. Vinitha Sree, S. Chattopadhyay, Y.U. Wenwei, A.P.C. Alvin, Application of recurrence quantification analysis for the automated identification of epileptic EEG signals, Int. J. Neural Syst. 21 (3) (2011) 199–211.

[5] U.R. Acharya, S. VinithaSree, A.P.C. Alvin, J.S. Suri, Application of non-linear and wavelet based features for the automated identification of epileptic EEG signals, Int. J. Neural Syst. 22 (2) (2012). 1250002-1-14.

[6] U.R. Acharya, F. Molinari, S. Vinitha Sree, S. Chattopadhyay, Ng. Kwan-Hoong, J.S. Suri, Automated diagnosis of epileptic EEG using entropies, Biomed. Signal Process. Control 7 (4) (2012) 401–408.

[7] U.R. Acharya, S. Vinitha Sree, J.S. Suri, Use of principal component analysis for automatic detection of epileptic EEG activities, Expert Syst. Appl. 39 (10) (2012) 9072–9078.

[8] U.R. Acharya, R. Yanti, G. Swapna, V.S. Sree, R.J. Martis, J.S. Suri, Automated diagnosis of epileptic electroencephalogram using independent component analysis and discrete wavelet transform for different electroencephalogram durations, Proc. Inst. Mech. Eng., Part H, J. Eng. Med. (2012), http://dx.doi.org/10.1177/0954411912467883.

[9] S. Altunay, Z. Telatar, O. Erogul, Epileptic EEG detection using the linear prediction error energy, Expert Syst. Appl. 37 (8) (2010) 5661–5665.

[10] R.G. Andrzejak, G. Widman, K. Lehnertz, C. Rieke, P. David, C.E. Elger, The epileptic process as nonlinear deterministic dynamics in a stochastic environment: an evaluation on mesial temporal lobe epilepsy, Epilepsy Res. 44 (2) (2001) 129–140.

[11] J. Arnhold, K. Lehnertz, P. Grassberger, C.E. Elger, A robust method for detecting interdependences: application to intracranially recorded EEG, Physica D 134 (4) (1999) 419–430.

[12] R. Aschenbrenner-Scheibe, T. Maiwald, M. Winterhalder, H.U. Voss, J. Timmer, A. Schulze-Bonhage, How well can epileptic seizures be predicted? An evaluation of a nonlinear method, Brain 126 (12) (2003) 2616–2626.

[13] K. Aslan, H. Bozdemir, C. Sahin, S.N. Ogulata, R. Ero, A radial basis function neural network model for classification of epilepsy using EEG signals, J. Med. Syst. 32 (5) (2008) 403–408.

[14] A. Babloyantz, C. Nicolis, J.M. Salazar, Evidence of chaotic dynamics of brain activity during the sleep cycle, Phys. Lett. 111A (1985) 152–157.

[15] D. Bai, T. Qiu, Li, The sample entropy and its application in EEG based epilepsy detection, J. Biomed. Eng. 24 (1) (2007) 200–205.

[16] C. Besthorn, H. Sattel, C. Geiger-Kabisch, R. Zerfass, H. Förstl, Parameters of EEG dimensional complexity in Alzheimer's disease, Electroen. Clin Neurophys. 95 (2) (1995) 84–89.

[17] Billauer's Peak Detection Algorithm. <http://billauer.co.il/peakdet.html> (last accessed 28.11.12).

[18] S. Boccaletti, C. Grebogi, Y.C. Lai, H. Mancini, D. Mazaet, The control of chaos: theory and applications, Phys. Rep. 329 (2000) 108–109.

[19] E. Bradley, Time-series analysis, in: M. Berthold, D. Hand (Eds.), Intelligent Data Analysis: An Introduction, Springer-Verlag, Berlin, 1999.

[20] D. Buck, G.A. Baker, A. Jacoby, D.F. Smith, D.W. Chadwick, Patients' experiences of injury as a result of epilepsy, Epilepsia 38 (4) (1997) 439–444.

[21] E. Callaway, P.R. Harris, Coupling between cortical potentials from different areas, Science 183 (4127) (1974) 873–875.

[22] K.C. Chua, V. Chandran, U.R. Acharya, C.M. Lim, Automatic identification of epileptic EEG signals using higher order spectra, J. Eng. Med. 223 (4) (2009) 485–495.

[23] K.C. Chua, V. Chandran, U.R. Acharya, C.M. Lim, Application of higher order spectra to identify epileptic EEG, J. Med. Syst. 35 (6) (2011) 1563–1571.

[24] D.J. Cross, J.E. Cavazos, The role of sprouting and plasticity in epileptogenesis and behavior, in: S. Schachter, G.L. Holmes, D.G. Trenite (Eds.), Behavioural Aspects of Epilepsy, Demos Medical Publishing, 2007, pp. 51–57.

[25] S. Dangel, P.F. Meier, H.R. Moser, S. Plibersek, Y. Shen, Time series analysis of sleep EEG, Comput. Assisted Phys. 14 (1999) 93–95.

[26] R.O. Duda, P.E. Hart, D.G. Stork, Pattern Classification, second ed., John Wiley & Sons Inc., 2006.

[27] J.P. Eckmann, S.O. Kamphorst, D. Ruelle, Recurrence plots of dynamical systems, Europhys. Lett. 4 (9) (1987) 973–977.

[28] R. Estellar, G. Vachtsevanos, J. Echauz, B. Litt, A comparison of fractal dimension algorithms using synthetic and experimental data, Proc IEEE Int Symp Circ Syst: Adaptive Digital Signal Process 3 (1999) 199–202.

[29] O. Faust, U.R. Acharya, L.C. Min, B.H. Sputh, Automatic identification of epileptic and background EEG signals using frequency domain parameters, Int. J. Neural Syst. 20 (2) (2010) 159–176.

[30] J. Feder, Fractals, Plenum Press, New York, 1988.

[31] J. Fell, J. Röschke, K. Mann, C. Schäffner, Discrimination of sleep stages: a comparison between spectral and nonlinear EEG measures, Electroen. Clin Neurophys. 98 (5) (1996) 401–410.

[32] W.J. Freeman, A proposed name for aperiodic brain activity: stochastic chaos, Neural Netw. 13 (1) (2000) 11–13.

[33] S. Ghosh-Dastidar, H. Adeli, Improved spiking neural networks for EEG classification and epilepsy and seizure detection, Integr. Comput.-Aided Eng. 14 (3) (2007) 187–212.

[34] S. Ghosh-Dastidar, H. Adeli, N. Dadmehr, Mixed-band wavelet-chaos-neural network methodology for epilepsy and epileptic seizure detection, IEEE Trans. Biomed. Eng. 54 (9) (2007) 1545–1551.

[35] S. Ghosh-Dastidar, H. Adeli, N. Dadmehr, Principal component analysis-enhanced cosine radial basis function neural network for robust epilepsy and seizure detection, IEEE Trans. Biomed. Eng. 55 (2) (2008) 512–518.

[36] S. Ghosh-Dastidar, H. Adeli, A new supervised learning algorithm for multiple spiking neural networks with application in epilepsy and seizure detection, Neural netw. 22 (10) (2009) 1419–1431.

[37] L. Glass, R.G. Michel, M.A. Mackey, A. Shrier, Chaos in neurobiology, IEEE Trans. Syst. Man Cybern. SMC 13 (5) (1983) 790–798.

[38] P. Grassberger, I. Procassia, Measuring the strangeness of strange attractors, Physica D 9 (1–2) (1983) 189–208.

[39] N.F. Guler, E.D. Ubey, I. Guler, Recurrent neural network employing Lyapunov exponents for EEG signals classification, Expert Syst. Appl. 29 (3) (2005) 506–514.

[40] L. Guo, D. Rivero, J.A. Seoane, A. Pazos, Classification of EEG signals using relative wavelet energy and artificial neural networks, in: Conf Proc of the First ACM/SIGEVO Summit on Genetic and, Evolutionary Computation, 2009, pp. 177–184.

[41] L. Guo, D. Rivero, A. Pazos, Epileptic seizure detection using multiwavelet transform based approximate entropy and artificial neural networks, J. Neurosci. Methods 193 (1) (2010) 156–163.

[42] L. Guo, D. Rivero, J. Dorado, J.R. Rabunal, A. Pazos, Automatic epileptic seizure detection in EEGs based on line length feature and artificial neural networks, J. Neurosci. Methods 191 (1) (2010) 101–109.

[43] L. Guo, D. Rivero, J. Dorado, C.R. Munteanu, A. Pazos, Automatic feature extraction using genetic programming: an application to epileptic EEG classification, Expert Syst. Appl. 38 (8) (2011) 10425–10436.

[44] T. Higuchi, Approach to an irregular time series on the basis of the fractal theory, Physics D 31 (2) (1988) 277–283.

[45] D. Hoyer, K. Schmidt, R. Bauer, U. Zwiener, M. Kohler, B. Luthke, M. Eiselt, Nonlinear analysis of heart rate and respiratory dynamics, IEEE Eng. Med. Biol. Mag. 16 (1) (1997) 31–39.

[46] N.E. Huang, Z. Shen, S.R. Long, M.C. Wu, H.H. Shih, Q. Zheng, N.C. Yen, C.H.H. Tung, H.H. Liu, The empirical mode decomposition and the Hilbert spectrum for nonlinear and nonstationary time series analysis, Proc. Roy. Soc. Lond. A 454 (1998) 903–995.

[47] L. Huang, Q. Sun, J. Cheng, Y. Huang, Prediction of epileptic seizures using bispectrum analysis of electroencephalograms and artificial neural network, in: Proceedings of the 25th Annual International Conference of the IEEE Engineering in Medicine and Biology Society, vol. 3, 2003, pp. 2947–2949.

[48] H.E. Hurst, Long-term storage of reservoirs: an experimental study, Trans. Am. Soc. Civ. Eng. 116 (1951) 770–799.

[49] L.D. Iasemidis, D.S. Shiau, J.C. Sackellares, P. Pardalos, Transition to epileptic seizures: optimization, in: D.Z. Du, P.M. Pardalos, J. Wang (Eds.), Discrete Mathematical Problems with Medical Applications, 'DIMACS Series in Discrete Mathematics and Theoretical Computer Science', vol. 55, American Mathematical Society, Providence, Rhode Island, 1999, pp. 55–74.

[50] L.D. Iasemidis, P. Pardalos, J.C. Sackellares, D. Shiau, Quadratic binary programming and dynamical system approach to determine the predictability of epileptic seizures, J. Comb. Optim. 5 (1) (2001) 9–26.

[51] L.D. Iasemidis, D.S. Shiau, J.C. Sackellares, P.M. Pardalos, A. Prasad, Dynamical resetting of the human brain at epileptic seizures: application of nonlinear dynamics and global optimization techniques, IEEE Trans. Biomed. Eng. 51 (3) (2004) 493–506.

[52] P. Jahankhani, V. Kodogiannis, K. Revett, EEG signal classification using wavelet feature extraction and neural networks, in: IEEE International Symposium on Modern Computing John Vincent Atanasoff, 2006, pp 120–124.

[53] Z. Iscan, Z. Dokur, D. Tamer, Classification of electroencephalogram signals with combined time and frequency features, Expert Syst. Appl. 38 (8) (2011) 10499–10505.

[54] B. Jelles, J.H. van Birgelen, J.P. Slaets, R.E. Hekster, E.J. Jonkman, C.J. Stam, Decrease of non-linear structure in the EEG of Alzheimer patients compared to healthy controls, Clin. Neurophysiol. 110 (7) (1999) 1159–1167.

[55] J. Jeong, J.H. Chae, S.Y. Kim, S.H. Han, Nonlinear dynamical analysis of the EEG in patients with Alzheimer's disease and vacular dementia, J. Clin. Neurophysiol. 18 (1) (2001) 58–67.

[56] H. Jing, M. Takigawa, Topographic analysis of dimension estimates of EEG and filtered rhythms in epileptic patients with complex partial seizures, Biol. Cybern. 83 (5) (2000) 391–397.

[57] T.-P. Jung, S. Makeig, M.J. McKeown, A.J. Bell, T.-W. Lee, T.J. Sejnowski, Imaging brain dynamics using independent component analysis, Proc IEEE 89 (7) (2001) 1107–1122.

[58] A.S. Kallimanis, S.P. Sgardelis, J.M. Halley, Accuracy of fractal dimension estimates for small samples of ecological distributions, Landscape Ecol. 17 (3) (2002) 281–297.

[59] N. Kannathal, C.M. Lim, U.R. Acharya, P.K. Sadasivan, Entropies for detection of epilepsy in EEG, Comput. Methods Programs Biomed. 80 (3) (2005) 187–194.

[60] N. Kannathal, U.R. Acharya, C.M. Lim, Q. Weiming, M. Hidayat, P.K. Sadasivan, Characterization of EEG: a comparative study, Comput. Methods Programs Biomed. 80 (1) (2005) 17–23.

[61] A.Y. Kaplan, Segmental structure of EEG more likely reveals the dynamic multistability of the brain tissue than the continual plasticity one, in: Proceedings of the Sixth International Conference on Neural information processing, vol. 2, 1999, pp. 633–638.

[62] J. Lamberts, P.L.C. Van den Broek, J. Bener, J. Van Egmond, R. Dirksen, A.M.L. Cohen, Correlation dimension of the human electroencephalogram corresponding to cognitive load, Neuropsychobiology 41 (3) (2000) 149–153.

[63] K. Lehnertz, C.E. Elger, Spatio-temporal dynamics of the primary epileptogenic area in temporal lobe epilepsy characterized by neuronal complexity loss, Electroencephalogr. Clin. Neurophysiol. 95 (2) (1995) 108–117.

[64] K. Lehnertz, C.E. Elger, Can epileptic seizures be predicted? Evidence from nonlinear time series analyses of brain electrical activity, Phys. Rev. Lett. 80 (22) (1998) 5019–5022.

[65] C.A. Lima, A.L. Coelho, M. Eisencraft, Tackling EEG signal classification with least squares support vector machines: a sensitivity analysis study, Comput. Biol. Med. 40 (8) (2010) 705–714.

[66] B.B. Mandelbrot, The Fractal Geometry of Nature, W.H. Freeman and Company, 1982.

[67] J. Martinerie, C. Adam, M. Le van Quyen, M. Baulac, B. Renault, F.J. Varela, Can epileptic crisis be anticipated?, Nat. Med. 4 (1998) 1173–1176.

[68] R.J. Martis, U.R. Acharya, J.H. Tan, A. Petznick, R. Yanti, K.C. Chua, E.Y.K. Ng, L. Tong, Application of empirical mode decomposition (EMD) for automated detection of epilepsy using EEG signals, Int. J. Neural Syst. 22 (6) (2012). 1250027-1-16.

[69] N. Marwan, N. Wessel, U. Meyerfeldt, A. Schirdewan, J. Kurths, Recurrence plot based measures of complexity and its application to heart rate variability data, Phys. Rev. E 66 (2) (2002) 026702.

[70] M. Molnár, G. Gács, G. Ujvári, J.E. Skinner, G. Karmos, Dimensional complexity of the EEG in subcortical Stroke: a case study, Int. J. Psychophysiol. 25 (3) (1997) 193–199.

[71] V.P. Nigam, D. Graupe, A neural-network-based detection of epilepsy, Neurol. Res. 26 (1) (2004) 55–60.

[72] C. Niederhoefer, F. Gollas, A. Chernihovskyi, K. Lehnertz, R. Tetzlaff, Detection of seizure precursors in the EEG with cellular neural networks, Epilepsia 45 (Suppl. 7) (2004) 245.

[73] C.L. Nikias, Higher-order spectral analysis, engineering in medicine and biology society, in: Proceedings of the 15th Annual International Conference of the IEEE, 1993, p. 319.

[74] H. Ocak, Automatic detection of epileptic seizures in EEG using discrete wavelet transform and approximate entropy, Expert Syst. Appl. 36 (2) (2009) 2027–2036.

[75] U. Orhan, M. Hekim, M. Ozer, EEG signals classification using the K-means clustering and a multilayer perceptron neural network model, Expert Syst. Appl. 38 (10) (2011) 13475–13481.

[76] I. Osorio, M.G. Frei, S.B. Wilkinson, Real-time automated detection and quantitative analysis of seizures and short-term prediction of clinical onset, Epilepsia 39 (6) (1998) 615–627.

[77] I. Osorio, M.G. Frei, B.F. Manly, S. Sunderam, N.C. Bhavaraju, S.B. Wilkinson, An introduction to contingent (closed-loop) brain electrical stimulation for seizure blockage, to ultra-short-term clinical trials, and to multidimensional statistical analysis of therapeutic efficacy, J. Clin. Neurophys. 18 (6) (2001) 533–544.

[78] R.J. Oweis, E.W. Abdulhay, Seizure classification in EEG signals utilizing Hilbert–Huang transform, Biomed. Eng. 10 (2011) 38.

[79] N. Paivinen, S. Lammi, A. Pitkanen, J. Nissinen, M. Penttonen, T. Gronfors, Epileptic seizure detection: a nonlinear viewpoint, Comput. Methods Programs Biomed. 79 (2) (2005) 151–159.

[80] C. Petitmengin, M. Baulac, V. Navarro, Seizure anticipation: Are neurophenomenological approaches able to detect pre-ictal symptoms?, Epilepsy Behav 9 (2) (2006) 298–306.

[81] F. Philippe, K. Henri, Is there chaos in the brain? Concepts of nonlinear dynamics and methods of investigation, Life Sci. 324 (2001) 773–793.

[82] J.P.M. Pijn, Quantitative Evaluation of EEG Signals in Epilepsy: Nonlinear Association Time Delays and Nonlinear Dynamics, Ph.D. Thesis, University of Amsterdam, 1990.

[83] J.P.M. Pijn, D.N. Velis, M.J. van der Heyden, J. DeGoede, C.W. van Veelen, F.H. Lopes da Silva, Nonlinear dynamics of epileptic seizures on basis of intracranial EEG recordings, Brain Topogr. 9 (4) (1997) 249–270.

[84] S.M. Pincus, Approximate entropy as a measure of system complexity, Proc Nat Acad Sci, USA 88 (1991) 2297–2301.

[85] S.M. Pincus, Assessing serial irregularity and its implications for health, Ann. N.Y. Acad. Sci. 954 (2001) 245–267.

[86] K. Polat, S. Gunes, Classification of epileptiform EEG using a hybrid systems based on decision tree classifier and fast Fourier transform, Appl. Math. Comput. 187 (2) (2007) 1017–1026.

[87] K. Polat, S. Gunes, Artificial immune recognition system with fuzzy resource allocation mechanism classifier, principal component analysis and FFT method based new hybrid automated identification system for classification of EEG signals, Expert Syst. Appl. 34 (3) (2008) 2039–2048.

[88] K. Polat, S. Gunes, A novel data reduction method: distance based data reduction and its application to classification of epileptiform EEG signals, Appl. Math. Comput. 200 (1) (2008) 10–27.

[89] N. Pradhan, D.N. Dutt, Data compression by linear prediction for storage and transmission of EEG signals, Int. J. Biomed. Comput. 35 (3) (1994) 207–217.

[90] W.S. Pritchard, D.W. Duke, Measuring chaos in the brain: a tutorial review of nonlinear dynamical EEG analysis, Int. J. Neurosci. 67 (1–4) (1992) 31–40.

[91] B. Qian, K. Rasheed, Hurst exponent and financial market predictability, in: IASTED Conference Financial Engineering and Applications, 2004, pp. 203–209.

[92] R.E. Ramsay, A.J. Rowan, A.M. Pryor, Special considerations in treating the elderly patient with epilepsy, Neurology 62 (Suppl. 2) (2004) S24–S29.

[93] P.E. Rapp, T. Bashore, J. Martinerie, A. Albano, I. Zimmerman, A. Mess, Dynamics of brain electrical activity, Brain Topogr. 2 (1–2) (1989) 99–118.

[94] P.E. Rapp, Chaos in the neurosciences: cautionary tales from the frontier, Biologist 40 (1993) 89–94.

[95] M. Rey, P. Guillemant, Contribution of non-linear mathematics (chaos theory) to EEG analysis, Neurophysiol. Clin. 27 (5) (1997) 406–428.

[96] J.S. Richman, M.J. Randall, Physiological time-series analysis using approximate entropy and sample entropy, Am. J. Physiol. Heart Circ. Physiol. 278 (2000) H2039–H2049.

[97] S.A.R.B. Rombouts, R.W.M. Keunen, C.J. Stam, Investigation of nonlinear structure in multichannel EEG, Phys. Lett. A 202 (5–6) (1995) 352–358.

[98] M. Rosenstein, J.J. Colins, C.J. De Luca, A practical method for calculating largest Lyapunov exponent from small data sets, Physica D 65 (1993) 117–134.

[99] N. Sadati, H.R. Mohseni, A. Magshoudi, Epileptic seizure detection using neural fuzzy networks, in: Proceedings of the IEEE International Conference on Fuzzy Systems, 2006, pp. 596–600.

[100] S. Schraag, U. Bothner, R. Gajraj, G.N. Kenny, M. Georgieff, The performance of electroencephalogram bispectral index and auditory evoked potential index to predict loss of consciousness during propofol infusion, Anesth. Analg. 89 (5) (1999) 1311–1315.

[101] M. Shen, F.H.Y. Chan, L. Sun, B. Beadle, Parametric bispectral estimation of EEG signals in different functional states of the brain, IEE Proc.: Sci. Meas. Technol. 147 (6) (2000) 374–377.

[102] J.W. Sleigh, E. Olofsen, A. Dahan, J. Goede de, A. Steyn-Ross, Entropies of the EEG: the effects of general anesthesia, in: Proceedings of the Fifth International Conference on Memory, Awareness and Consciousness, USA, 2001.

[103] V. Srinivasan, C. Eswaran, N. Sriraam, Artificial neural network based epileptic detection using time-domain and frequency domain features, J. Med. Syst. 29 (6) (2005) 647–660.

[104] V. Srinivasan, C. Eswaran, N. Sriraam, Approximate entropy-based epileptic EEG detection using artificial neural networks, IEEE Trans. Inform. Technol. Biomed. 11 (3) (2007) 288–295.

[105] C.J. Stam, T.C. Van Woerkom, R.W.M. Keunen, Non-linear analysis of the electroencephalogram in Creutzfeldt–Jakob disease, Biol. Cybern. 77 (4) (1997) 247–256.

[106] C.J. Stam, E.M.H. van der Leij, R.W.M. Keunen, D.L.J. Tavy, Nonlinear EEG changes in postanoxic encephalopathy, Theor. Biosci. 118 (1999) 209–218.

[107] C.J. Stam, J.P. Pijn, P. Suffczynski, Lopez da Silva FH. Dynamics of the human alpha rhythm: evidence for nonlinearity?, Clin Neurophysiol. 110 (10) (1999) 1801–1803.

[108] K.M. Stein, N. Lippman, P. Kligfield, Fractal rhythms of the heart, J. Electrocardiol. 24 (1992) 72–76.

[109] A. Subasi, EEG Signal classification using wavelet feature extraction and a mixture of expert model, Expert Syst. Appl. 32 (4) (2007) 1084–1093.

[110] A. Subasi, M.I. Gursoy, EEG Signal classification using PCA, ICA, LDA and support vector machine, Expert Syst. Appl. 37 (12) (2010) 8659–8686.

[111] D.P. Subha, P.K. Joseph, U.R. Acharya, C.M. Lim, EEG signal processing: a survey, J. Med. Syst. 34 (2) (2010) 195–212.

[112] J. Theiler, Spurious dimension from correlation algorithms applied to limited time-series data, Phys. Rev. A 34 (3) (1986) 2427–2432.

[113] J. Theiler, S. Eubank, A. Longtin, B. Galdrikian, J.D. Farmer, Testing for nonlinearity in time series: the method of surrogate data, Physica D 58 (1–4) (1992) 77–94.

[114] A.T. Tzallas, M.G. Tsipouras, D.I. Fotiadis, Automatic seizure detection based on time-frequency analysis and artificial neural networks, Comput. Intell. Neurosci. (2007). http://dx.doi.org/10.1155/2007/80510.

[115] E.D. Ubeyli, I. Güler, Spectral analysis of internal carotid arterial Doppler signals using FFT, AR, MA, and ARMA methods, Comput. Biol. Med. 34 (4) (2004) 293–306.

[116] E.D. Ubeyli, Least squares support vector machine employing model-based methods coefficients for analysis of EEG signals, Expert Syst. Appl. 37 (1) (2010) 233–239.

[117] A.E. Villa, I.V. Tetko, Cross-frequency coupling in mesiotemporal EEG recordings of epileptic patients, J. Physiol. 104 (3–4) (2010) 197–202.

[118] M. Vitterli, Wavelet and filter banks: theory and design, IEEE Trans. Signal Process. 40 (9) (1992) 2207–2232.

[119] J. Wackermann, Beyond mapping: estimating complexity of multi-channel EEG recordings, Acta Neurobiol. Exp. 56 (1) (1996) 197–208.

[120] D. Wang, D. Miao, C. Xie, Best basis-based wavelet packet entropy feature extraction and hierarchical EEG classification for epileptic detection, Expert Syst. Appl. 38 (11) (2011) 14314–14320.

[121] C.L. Webber Jr., J.P. Zbilut, Dynamical assessment of physiological systems and states using recurrence plot strategies, J. Appl. Physiol. 76 (2) (1994) 965–973.

[122] P.D. Welch, The use of fast Fourier transform for the estimation of power spectra: a method based on time averaging over short, modified periodograms, IEEE Trans. Audio Electroacoust. AU-15 (1967) 70–73.

[123] A. Wolf, J.B. Swift, H.L. Swinney, J.A. Vastano, Determining Lyapunov exponents from a time series, Physica D 16 (1985) 285–317.

[124] World Health Organization, Epilepsy. <http://www.who.int/mental_health/neurology/epilepsy/en/index.html> (last accessed 28.11.12).

[125] J.J. Wright, D.T.J. Liley, Dynamics of the brain at global and microscopic scales. Neural networks and the EEG, Behav. Brain Sci. 19 (1996) 285–320.

[126] D. Yao, Electroencephalography inverse problem by subspace decomposition of the fourth-order cumulant matrix, J. Biomed. Eng. 17 (2) (2000) 174–178.

[127] J.P. Zbilut, C.L. Webber Jr., Embeddings and delays as derived from quantification of recurrence plots, Phys. Lett. A 171 (3–4) (1992) 199–203.

[128] S.M. Zhuo, J.Q. Gan, F. Sepulveda, Classifying mental tasks based on features of higher-order statistics from EEG signals in brain– computer interface, Inf Sci 178 (6) (2008) 1629–1640.

[129] H. Adeli, Z. Zhou, N. Dadmehr, Analysis of EEG records in an epileptic patient using wavelet transform, J. Neurosci. Methods 123 (1) (2003) 69–87.

[130] H. Adeli, S. Ghosh-Dastidar, (in corroboration with Nahid Dadmehr), Automated EEG-based Diagnosis of Neurological Disorders - Inventing the Future of Neurology, CRC Press, Taylor & Francis, Boca Raton, Florida, 2010.

[131] M. Ahmadlou, H. Adeli, Wavelet synchronization methodology: A new approach for EEG-based diagnosis of ADHD, Clin. EEG Neurosci. 41 (1) (2010) 1–10.

[132] M. Ahmadlou, H. Adeli, Fuzzy synchronization likelihood with application to attention deficit hyperactivity disorder, Clin. EEG Neurosci. 42 (1) (2011) 6–13.

[133] M. Ahmadlou, H. Adeli, Graph theoretical analysis of organization of functional brain networks in ADHD, Clin. EEG Neurosci. 43 (1) (2012) 5–13.

[134] M. Ahmadlou, H. Adeli, A. Adeli, Improved visibility graph fractality with application for diagnosis of Autism Spectrum Disorder, Phys. Stat. Mech. Appl. 391 (20) (2012) 4720–4726.

[135] M. Ahmadlou, H. Adeli, A. Adeli, Fuzzy synchronization likelihood-wavelet methodology for diagnosis of Autism Spectrum Disorder, J. Neurosci. Methods 211 (2) (2012) 203–209.

[136] M. Ahmadlou, H. Adeli, A. Adeli, Fractality and a Wavelet-Chao Methodology for EEG-based diagnosis of Alzheimer's Disease, Alzheimer Dis. Assoc. Disord. 25 (1) (2011) 85–92.

[137] Z. Sankari, H. Adeli, Probabilistic neural networks for EEG-based diagnosis of Alzheimer's disease using conventional and wavelet coherence, J. Neurosci. Methods 197 (1) (2011) 165–170.

[138] Z. Sankari, H. Adeli, A. Adeli, Intrahemispheric, interhemispheric and distal EEG coherence in Alzheimer's disease, Clin. Neurophysiol. 122 (5) (2011) 897–906.

[139] Z. Sankari, H. Adeli, A. Adeli, Wavelet Coherence Model for Diagnosis of Alzheimer's Disease, Clin. EEG Neurosci. 43 (3) (2012) 268–278.

[140] M. Ahmadlou, H. Adeli, A. Adeli, Fractality analysis of frontal brain in Major Depressive Disorder, Int. J. Psychophysiol. 85 (2) (2012) 206–211.

[141] M. Ahmadlou, H. Adeli, A. Adeli, Spatio-Temporal Analysis of Relative Convergence (STARC) of EEGs reveals differences between brain dynamics of depressive women and men, Clin. EEG Neurosci. 44 (2013).